technische universität
dortmund

2014

SCIENTIFIC HIGHLIGHTS

Annual Report

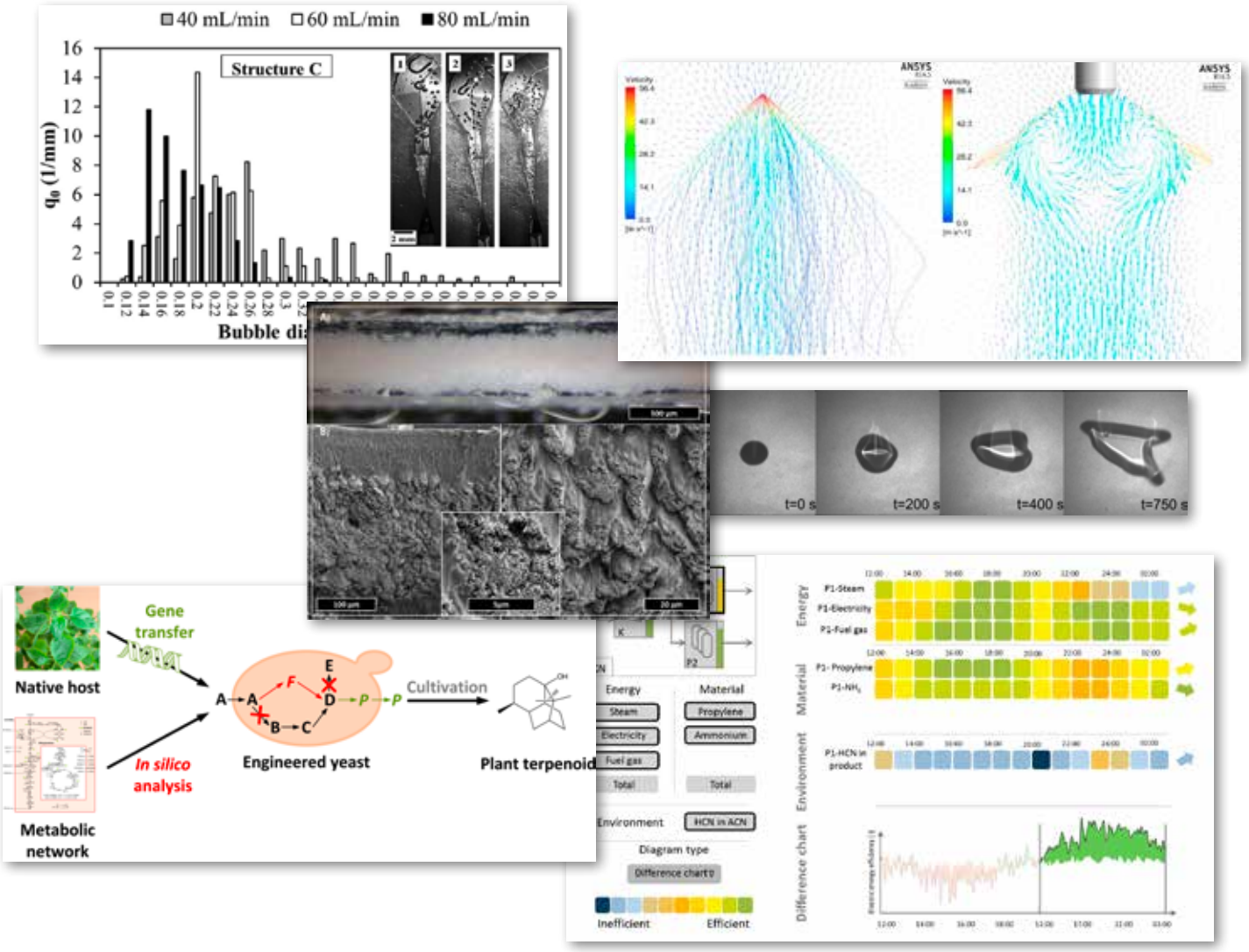

Fakultät Bio- und
Chemieingenieurwesen

Content

Content

Department of BCI

Preface

Dear Reader,

It's my pleasure to introduce the 5th volume of the Scientific Highlights of the Faculty of Bio- and Biochemical Engineering. The year 2014 has been very productive and numerous scientific success stories have been written. A selection of those is presented in this issue. Comparing the Scientific Highlights of the past years gives a nice overview over the scientific development of the different groups. Also changes of faculty members have a great influence on the scientific profile of BCI. Prof. Walzel has retired 2014 and Prof. Schmid has moved to the UFZ Leipzig in the same year. We are excited to see how their successors will fill the great gaps left by both scientists.

Scientific Highlights in such a highly interdisciplinary and application oriented faculty as BCI are not produced by professors and group leaders but by our students, PhD. students and postdocs. Those come from all over the world and have not only chemical or biochemical engineering background, but are physicists, chemists, biologists, pharmacists, mathematicians, and others. Thank you. The second basis of our success is the strong support we get from our technicians and our chair and department administrations. We are very grateful for that.

As every year, I hope that this brochure attracts the interest of students to join our research groups and academic as well as industrial researchers to find collaboration partners here.

Enjoy the reading,

Joerg Tiller

Equipment Design (AD)

Process intensification through microstructured helically coiled tubular devices

Safa Kutup Kurt, Norbert Kockmann

Process intensification via miniaturization has become an attractive research field for industry and R&D especially for the production of fine chemicals and pharmaceuticals. Additionally, small-scale equipment enables rapid process development in the lab with consistent scale-up capability. Tubular devices with dedicated arrangement are cost-efficient and reliable and can serve for different purposes.

The motivation of the miniaturization is to gain the advantage of large surface area to volume ratios, i.e. large specific surface area, which can enhance the mass and heat transport in a process. In this manner, several microstructured devices (microreactors) have been developed by researchers and their heat and/or mass transfer characterization have been either experimentally investigated or simulated via computer aided tools in laminar flow regimes. Due to the laminar flow profile, axial dispersion of the fluid elements is increased along the microreactor. Therefore, besides the limitation of heat transfer, residence time distribution (RTD) of the microreactor is also limited to laminar flow profile, which results in low selectivity of the product, if a complex chemical reaction system is subjected to be applied.

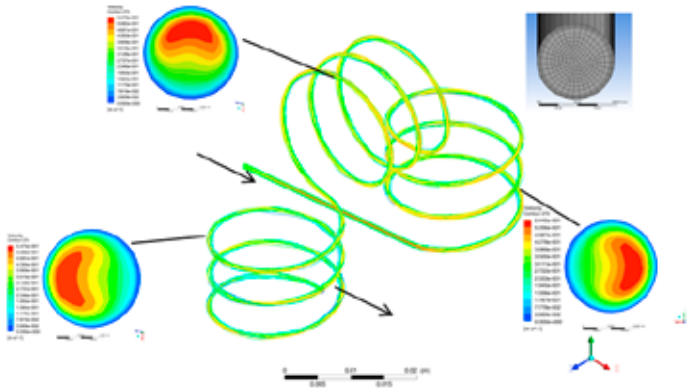

Figure 1: Cross-sectional velocity profiles, which are obtained by computational fluid dynamics (CFD) simulation, within a microstructure coiled flow inverter.

Helically coiled tubular devices (HCTD) offer improved radial mixing due to the secondary flow profile, i.e. Dean flow, which is maintained by the effect of centrifugal force that acts perpendicular to the flow direction of the fluid elements. As a result, relatively narrow RTD can be achieved even at laminar flow regimes. In the content of this project, a type of HCTD, i.e. coiled flow inverter (CFI), which offers the narrowest RTD in laminar flow regimes, is fabricated in micro-scale for process intensification. Radial mixing can be further enhanced within the CFI, as the Dean flow can be inversed on the tube cross-section by applying 90°-bends (Figure 1). In order to gain a degree of freedom regarding reactor placement, different configuration of CFI reactors are arranged as it is presented in Figure 2.

Contact:
Safa-Kutup.Kurt@bci.tu-dortmund.de
Norbert.Kockmann@bci.tu-dortmund.de

RTD of these configurations were experimentally investigated and the results were compared with the conventional CFI configuration. As it can be seen from Figure 3, different configurations of CFI reactor show similar results in terms of RTD and thus one of these configurations can be chosen depending on the purpose of an application.

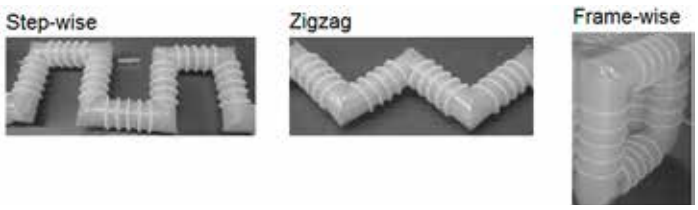

Figure 2: Different configurations of microstructured CFI reactors, i.e. step-wise, zigzag, and frame-wise for the purpose of an application and/or place requirement.

Systematic design approach of a best performance CFI reactor in terms of RTD can be utilized in order to fabricate a CFI reactor for given flow rate and residence time on lab, pilot, and production scale applications. Hence, CFI reactor is also a promising concept towards modularization.

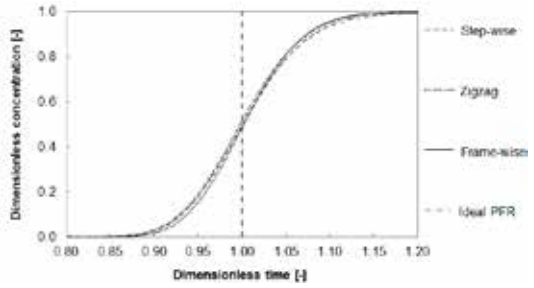

Figure 3: Residence time distribution curves of different microstructured CFI reactor configurations, which were obtained experimentally for identical reactor geometries (inner tube diameter is 0.5 mm, inner volume of the reactors is 2.35 mL) in comparison with RTD of an ideal plug flow reactor (PFR). Volumetric flow rate is 3 mL/min with Re = 143.

Publications:
J. Singh, N. Kockmann, K.D.P. Nigam, Novel three-dimensional microfluidic device for process intensification, Chem. Eng. Proc., 86, 78-89, 2014

M.G. Gelhausen, S.K. Kurt, N. Kockmann, Mixing and Heat Transfer in Helical Capillary Flow Reactors with Alternating Bends, ASME-ICNMM2014-21779, V001T13A001, 2014

S.K. Kurt, N. Kockmann, Design of a milli/microstructured coiled flow inverter as a plug flow reactor in laminar flow, IMRET13, Budapest, 23. - 25. June, 2014

M.G. Gelhausen, S.K. Kurt, N. Kockmann, Highly exothermic reaction in short helical alternating reactor capillaries with laminar flow, IMRET13, Budapest, 23. - 25. June, 2014

Chemisorption at Small Levitated Single Bubbles

Alexander Tollkötter, Lukas Hohmann, Norbert Kockmann

For dimensioning of conventional multiphase equipment, mass transfer has to be investigated between bubble swarms or even single bubbles surrounded by liquid. In our research, a new device was constructed to levitate bubbles with hydraulic diameters of 0.1 to 2.5 mm. Goal was to investigate mass transfer at bubbles on the microscale.

To observe gas bubbles in a nearly steady state, a measurement device was designed and installed consisting of a glass channel with an expanding quadratic cross-section. A drawing with its components and a cut through the main channel are given in Figure 1. Single bubbles were precisely injected with a µL-syringe into a downward liquid flow.

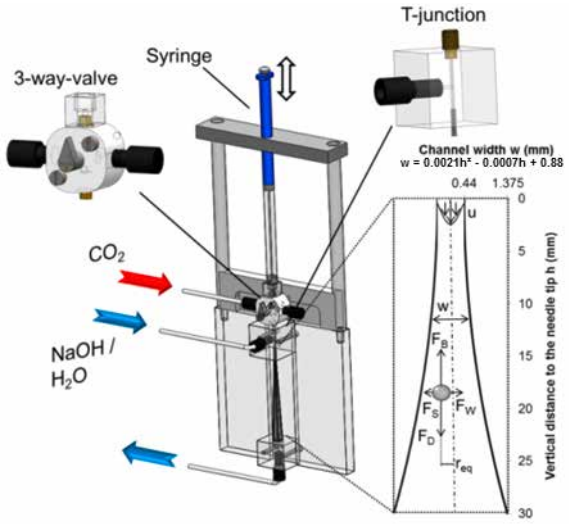

Figure 1: Drawing of the constructed device and a sketch of the inside of the glass channel.

Due to the equilibrium of rising and drag forces, the bubble levitated at a height corresponding to the liquid flow rate. Tailored drag correlations for our device were determined with reference to literature models to calculate the levitation position appropriately. It was quite easy to catch bubbles for a wide range of different liquid flow rates and bubble diameters due the reducing velocity based on diameter enlargement and continuity. Nitrogen was absorbed within the surrounding liquid and, hence bubble diameters decreased with a constant, nearly identical negative slope indicating a similar dissolving speed of all bubble diameters and water purities independent of the starting diameters. For carbon dioxide, bubble diameters stayed constant after a rapid decrease from the start for saturated water as presented in Figure 2.

The constant value was reached as equilibrium of saturated solution and identical partial pressures of the impurities in the bubble due to desorption processes of solved nitrogen within the liquid. Modeling of the mass transfer showed good similarities with adaption of the inlet purity of carbon dioxide.

Chemisorption in alkaline solutions resulted in steeper slopes of the curves as a consequence of superimposed chemical reaction and higher concentration gradients. Comparison of common literature models of mass transfer coefficients and the experimental data showed similarities assuming rigid surfaces of the bubbles. Furthermore, the influence of precipitation of $BaCO^3$ from BaOH solution showed a decreasing mass transfer coefficient even chemical reaction took place, which was referred to an additional resistance due to the solids on the bubble's surface based on observed encapsulation.

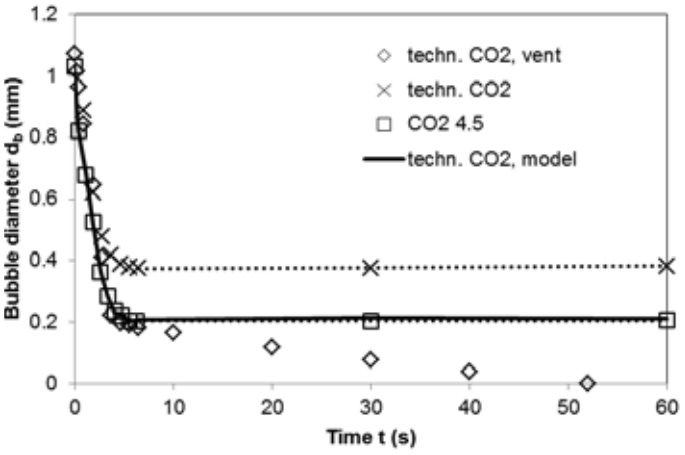

Figure 2: Decreasing bubble diameters of different gas purities within aqueous solutions.

In summary, mass transfer processes of single microbubbles were studied at the interface of a two- or three-phase system with variable observation times.

Publications:
A. Tollkötter, N. Kockmann, Absorption and Chemisorption of a Small Levitated, Single Bubbles in Aqueous Solutions, MPDI Processes 2014, 2, 200-215; doi:10.3390/pr2010200

L. Hohmann, A. Tollkötter, N. Kockmann, Mass transfer and precipitation at the gas-liquid interface of single, levitated microbubbles, IMRET13, Budapest, 23.-25.06.2014

L. Hohmann, A. Tollkötter, F. Schilling, M. Matuschek, N. Kockmann, Visualization of Particle Formation Process at the Gas-liquid Interface in Continuous-Flow Devices, International Workshop on Nucleation and Early Stages of Particle Formation, Erlangen, 05.-06.06.2014

Contact:
Alexander.Tollkötter@bci.tu-dortmund.de
Lukas.Hohmann@bci.tu-dortmund.de
Norbert.Kockmann@bci.tu-dortmund.de

Process intensification in extraction processes

Alexander Holbach, Norbert Kockmann

The Laboratory of Equipment Design has developed an intensified, miniaturized stirred-pulsed extraction column with inner diameter of 15 mm and modular sections of 220 mm height consisting of 10 stirred cells. The stirred cells enable high energy input, and therefore high specific surface and good extraction efficiencies up to 25 equilibrium stages per meter column height for investigated test systems.

Understanding of hydrodynamics in the column is the base for successful applications with high separation efficiency. Beside good dispersion, low backflow is crucial. The backflow was minimized with narrow plates between the cells. Hence, the dispersed phase coalesces at the plates that separate the stirred cells. The coalescence area is destroyed by continuous pulsation of the fluid column, which transports the dispersed phase into the next stirred cell. The fluid dynamics and mass transfer inside the column were characterized with the EFCE - test system water (continuous)/acetone/n-butylacetate (dispersed). We achieved a dispersed phase hold up inside the active extraction part up to 50%, and a specific surface of more than 3000 m^2/m^3.The extraction efficiency was measured to 17 and 25 stages per meter for the mass transfer direction (d → c) and (c → d), respectively. The comparison with other conventional pilot plant columns shows high extraction efficiency, but also a loss in total throughput.

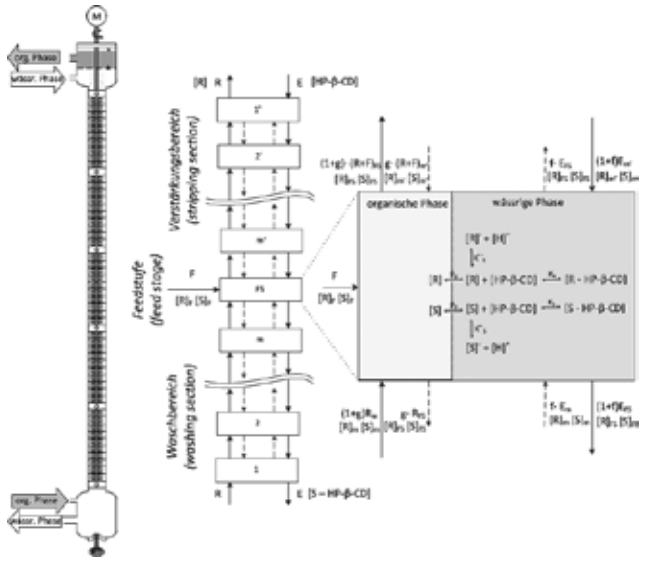

Figure 1: Fractional extraction of a-cyclohexyl mandelic aced with cyclodextrin, modeled with backflow model.

The characterization of the hydrodynamics and mass transfer of a stirred-pulsed millistructured column shows the opportunities and limits of the process intensification of miniaturized extraction columns. Optical analysis reveals small droplets in the range of 0.4–1.5 mm for the stirring area. The coalescence area has bigger droplets in the range of 0.5–1.7 mm. It was shown that the mass transfer direction from (c → d) is coalescence inhibited and produces generally smaller droplets, but also lower total throughput. Depending on the smaller droplets, the highest specific surface can be observed for the mass transfer direction (c → d) with an S/V-ratio of 3177 m^2/m^3. The specific surface within the active extraction part is in the same range as values given in literature to capillary micro contactors. Higher total throughputs and stirrer speeds around 900 rpm result in better extraction efficiencies. The process intensification enables many theoretical stages per meter in small process volume. This enables the separation of complex mixtures such as the purification of chiral molecules.

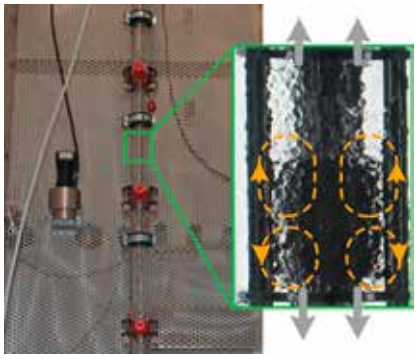

The equipment offers new possibilities for the laboratory and opportunities in process development, which bridges the gap for extraction tasks between the batch chemistry and the continuously operated plants.

Publications:
D. Jaritsch, A. Holbach, N. Kockmann, Counter-current Extraction in Microchannel Flow: Current Status and Perspectives, Trans. ASME J. Fluids Eng. 136, 091211, September 2014, doi:10.1115/1.4026608

A. Holbach, E. Caliskan, H.S. Lee, N. Kockmann, Process Intensification in Small Scale Extraction Columns for Counter-Current Operations, Chem. Eng. & Proc. - PI, 80, 21–28, 2014

A. Holbach, D. Jaritsch, J. Godde, N. Kockmann, Prozessentwicklung in miniaturisierten Laborkolonnen am Beispiel der Enantioselektiven Extraktion, Chem. Ing. Techn. 86, 621-629, 2014

Contact:
alexander.holbach@bci-tu-dortmund.de
kockmann@bci.tu-dortmund.de

Acceleration of modular plant design by systematic reactor selection from equipment pools

Lukas Hohmann, Nikolai Krasberg (INVITE GmbH, Leverkusen), Thomas Bieringer (INVITE), Norbert Kockmann

Continuous production plants are state of the art for large-scale chemical processes as they offer major advantages according to productivity, process safety, efficiency and product quality (steady-state operation and a high degree of automation). The production of specialties, life science products and pharmaceuticals is usually carried out in batch mode. Nonetheless, the interest on continuous production concepts rises in the branches.

Modular plant design is widely discussed as a key concept for achieving flexibility in continuous production and accelerated process realization (time to process). In this vison, a modular plant consists of multiple elements (modules), representing a unit operation (e.g. reaction, separation) or process functions (e.g. pumping, heat exchange), each. Modules can be arranged flexibly to form a plant (Figure 1). Moreover, the modules are fully engineered, characterized and documented, which reduces planning effort Therefore, processes can be adapted quickly to higher/lower production capacities or to new products from the same product family.

Figure 1 Modular plant in a process container.

In this project, a systematic selection concept for flow reactors from a pool of pre-defined reactors systems was developed. With short-cut models the technical suitability of typical reactors is evaluated. So-called 'interconnection matrices' are generated for each reactor system in the pool (Figure 2). Availability of reactor elements and options for in-series connection and numbering-up are considered.

All possible interconnections are regarded as a reactor setup. Using a computer-aided approach, all setups from each matrix are evaluated by mathematical models (technical criteria). These criteria are based on chemical engineering considerations (e.g. residence time, pressure drop, heat transfer, stability of the chemical system and runaway behavior), while equipment data (e.g. channel diameter, volume, pressure drop and heat transfer characteristics) is combined with process conditions (e.g. flow rate, temperature, concentration level) and physical/chemical properties of the system (e.g. viscosity, heat capacity, reaction kinetics).

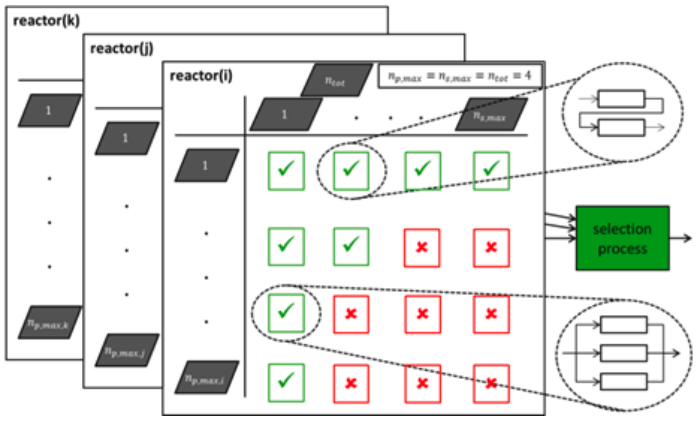

Figure 2: Interconnection matrices for reactors from an equipment pool.

Publications:
N. Krasberg, L. Hohmann, T. Bieringer, C. Bramsiepe, N. Kockmann, Selection of technical reactor equipment for modular, continuous small scale plants, MPDI Processes 2014, 2, 265-292; doi:10.3390/pr2010265

C. Bramsiepe, N. Krasberg, C. Fleischer, L. Hohmann, N. Kockmann, G. Schembecker, Information technologies for innovative process and plant design, Chemie-Ingenieur-Technik, 86, 966-981, 2014; DOI: 10.1002/cite.201400029

N. Krasberg, L. Hohmann, S. Falß, N. Kockmann, Facilitating the scale-up of flow processes using a computer-aided selection of reactor equipment, IMRET13, Budapest, 23.-25.06.2014

Contact:
Lukas.Hohmann@bci.tu-dortmund.de
Norbert.Kockmann@bci.tu-dortmund.de

The sequence of criteria is ordered by the amount of information, being required for the corresponding short-cut model. Thus, the selection approach can assist process development from the very early stages (poor availability of information) up to detail engineering and realization. In the last step of the procedure, a simulation of technically suitable reactor setup is conducted (Figure 3).

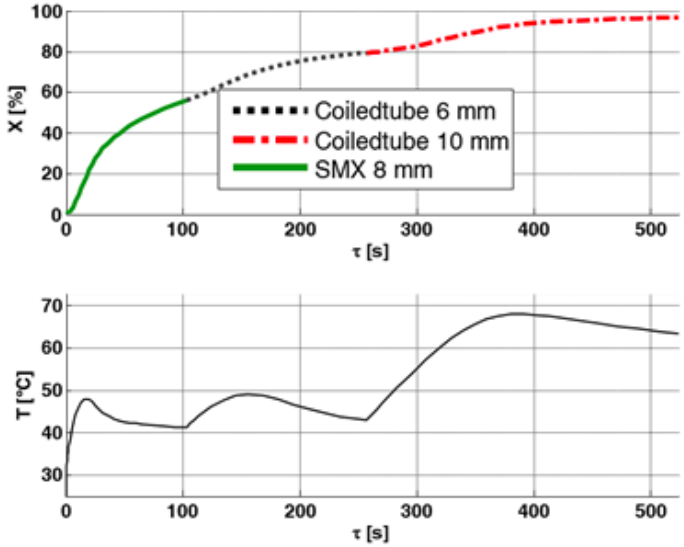

Figure 3: Short-cut simulation (conversion X and temperature T profiles) of a selected, technical feasible reactor concept which consists of multiple reactor systems. The hazardous synthesis of an ionic liquid was used as an example process.

Plant and Process Design (APT)

Selection of Aqueous Two-Phase Systems for use in Centrifugal Partition Chromatography

Christoph Schwienheer, Juliane Merz, Gerhard Schembecker

Centrifugal partition chromatography (CPC) is a kind of liquid-liquid chromatography, whereby one phase is kept stationary in chambers by a centrifugal field, while flown through by the other, so called, mobile phase. The selection of suitable biphasic phase systems is thereby of crucial importance. Aqueous-organic systems have been widely used for the separation of natural products and lot of knowledge about the selection of suitable systems and operation conditions of CPC is available. Aqueous two phase systems (ATPS) can be used to offer the possibility to purify biotechnological substances like proteins. However, the selection and use of ATPS in CPC and the selection of appropriate operation conditions have rarely been investigated yet. In the following, the selection of suitable ATPS and operation conditions for efficient separations of biomolecules in CPC is determined. Therefore, the hydrodynamic in the CPC chambers, the possibility to adjust the partition coefficient of the target compounds and the stability of biochemical compounds against denaturation during the CPC run were researched.

Regarding the ATPS selection for use in CPC, it is mainly important to retain the stationary phase in the chambers. This is determined by the flow pattern, which depends on the phase system's properties and the operating conditions of the CPC. Phase systems can be regarded as "unstable", if stationary phase is bleeding even at very low mobile phase volume flows and hence decreasing the amount of stationary phase in the chambers. These systems will be inefficient when used in CPC and more "stable" systems which allow higher stationary phase retention and the use of higher volume flows will be more efficient for CPC separation. Exemplarily, the flow pattern for three different ATPS at a depicted CPC operating point, i.e. rotational speed and mobile phase volume flow is shown in figure 1, wherein stationary phase is dyed dark. ATPS 1 can be considered as unstable compared to systems 2 and 3, as the amount of stationary phase in hydrodynamic equilibrium is low ("white" areas represent mobile phase are large), even at low volume flow of mobile phase. System 2 was selected more distanced to the critical point (increased ratio of phase forming compounds) with the phases becoming more different in their physicochemical properties. Significant higher mobile phase volume flows could be operated. System 3 was selected with a higher molecular weight of PEG also showing a good possibility to retain stationary phase, but the volume flow range applicable was less as for system 2. Thus, system 2 should be chosen as appropriate and stable system.

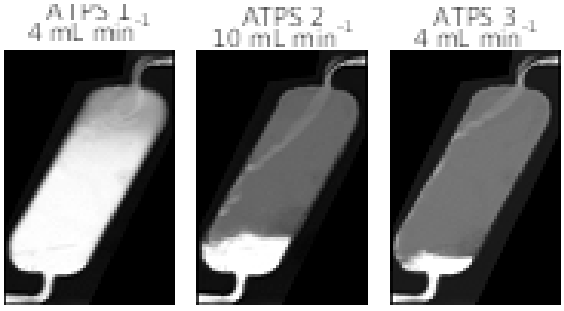

Figure 1: Flow pattern of three different ATPS at selected operating point of the CPC (1200 rpm). Stationary phase is dyed black.

Beside the flow pattern, the partition coefficient of the target compound(s) has to be in a suitable range and the solubility of compounds needs to be sufficiently high in order to operate the CPC efficiently. When selecting a phase system for CPC, it has to be checked if these restrictions are fulfilled or can be adjusted. Therefore, we investigated the possibility to adjust the partition coefficient of several proteins, representative for biochemical compounds. It was found, that the partition coefficient can be adjusted by changing the pH value of the ATPS or by addition of displacement salts. However, if the restrictions cannot be fulfilled by these adjustments, the ATPS system itself might have to be changed to a less stable system, because the phases become more equal and partition coefficients suitable for CPC separation are more easily adjustable.

All results concerning the selection and use of ATPS and CPC operating conditions were summarized in Schwienheer et al. 2014 as a guideline for future process design.

Contact:
christoph.schwienheer @bci.tu-dortmund.de
juliane.merz@bci.tu-dortmund.de
gerhard.schembecker@bci.tu-dortmund.de

Publications:
C. Schwienheer, J. Merz, G. Schembecker, J. Liq. Chromatogr. Related Technol. DOI: 10.1080/10826076.2014.951765 (2014).

Intensified hydroformylation as an example for flexible intermediates production

Development of an optimized kinetic model considering different reaction conditions

Tim Seifert, Phanuel Fakner, Stefan Sievers, Frank Stenger, Bart Hamers, Markus Priske, Marc Becker, Robert Franke, Gerhard Schembecker and Christian Bramsiepe

One of the future challenges for chemical engineering is the design of flexible production plants allowing an adaptation of production output to an uncertain market development. Consequently, the target for the design of new processes must be the identification of equipment allowing for a capacity expansion close to market development. On the example of hydroformylation we compared a conventional and an intensified process design in terms of the ability to cope with changing market conditions. The intensified design consisted of a jet loop reactor followed by a membrane section to separate and recycle the homogenous catalyst. We found that technologies like membrane processes, which require numbering-up to achieve full scale production capacity, are especially suitable for stepwise capacity expansion and offer substantial economic benefit in comparison to conventional technologies.

In our investigation we compared a conventional hydroformylation plant, which uses a bubble column reactor and distillation sequence with an intensified setup, where the catalyst is rejected and recycled with the help of ONF membranes. In addition jet loop reactors are used to improve selectivity and conversion compared to the bubble column applied in the conventional process. For the comparison of the intensified and the conventional process we investigated two major aspects: the effect of process intensification on the overall process economy and the flexible adaptation of production capacity to market development. For both aspects we evaluated whether the intensified equipment allows for a cost effective capacity expansion. Assuming that both processes are installed with full design capacity and without capacity expansion, we compared first compared the conventional plant to the intensified process by discounted cash flow (DCF) analysis.

Figure 1 shows the benefit of the intensified process. The modified process design leads to an NPV improvement of more than 30% compared to the conventional plant. The improvement is a direct result of the reduction in raw material consumption; especially propene consumption could be reduced by application of intensified equipment.

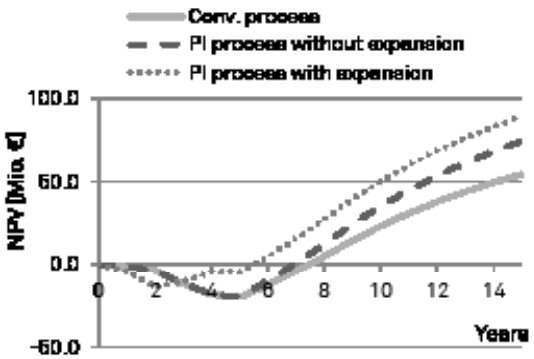

Figure 1: DCF diagram of conventional and PI plant if total capacity is installed at production start-up, compared with capacity expansion.

Beyond the direct advantages resulting from improved process performance of the intensified setup, we investigated the benefits resulting from a potential stepwise capacity expansion of the intensified process. Due to the fact that both, jet loop reactors and membrane units, are technically limited to certain maximum dimensions, numbering up is required to reach design capacity. These unit operations are thus predestined for modular design and offer the opportunity for a stepwise plant expansion, entering market with a reduced setup. To demonstrate the benefit of an earlier production start, the point of market entry could be shifted from year four when the conventional equipment was applied to year two using the intensified technology. Thus only half of the final capacity was installed initially. An expansion of the plant setup was carried out in year four where the upper bound of the operating range of the initially installed setup was reached. As shown in Figure 1, the option to allow an earlier production start leads to an increased NPV of 89 M € which is 16% higher compared to the PI plant without expansion. Thus, it could be demonstrated that an early market entry could be realized by the application of modularized and intensified process equipment, preparing substantial economic benefits compared to the application of conventional production technology. In summary, it could be demonstrated that the intensified hydroformylation technology was economically beneficial and allowed for an adaptation of production capacity to the market development. Consequently, the investment risk was reduced, which could be enhanced by additionally splitting capacity expansion.

Publications:
T. Seifert, P. Fakner, S. Sievers, F. Stenger, B. Hamers, M. Priske, M. Becker, R. Franke, G. Schembecker, C. Bramsiepe, Chem. Eng. Process. Process Intensif.
doi:10.1016/j.cep.2014.07.003 (2014).

Contact:
christian.bramsiepe@bci.tu-dortmund.de
gerhard.schembecker@bci.tu-dortmund.de

Biomaterials and Polymer Science (BMP)

Organosoluble Artificial Metalloenzymes

Polymer Enzyme Conjugates as Chiral Ligands for Sharpless Dihydroxylation of Alkenes in Organic Solvents

Melanie Leurs, Stefan Konieczny, Jörg C. Tiller

Enzymes are becoming a serious alternative to organometallic catalysts in the synthesis of fine chemicals. There is a great variety of chemical reactions that can be catalyzed by enzymes, particularly when working in organic solvents. However, many reactions cannot be catalyzed by enzymes. In order to enhance the reaction spectrum of enzymes in organic solvents, we modified the active center of organosoluble poly(2-methyloxazoline)-enzyme-conjugates with osmate to create artificial enzymes that are capable of catalyzing the dihydroxylation of alkenes with high enantioselective control in organic solvents. These catalysts are the first examples of organosoluble artificial metalloenzymes.

Artificial metalloenzymes (AMEs) have are an emerging field in catalysis. So far no organosoluble examples are known, which greatly restricts the use of such systems. In general, AMEs are merging molecular recognition ability of proteins and broad reactivity scope of organometallic catalysts to form superior hybrid catalysts. We chose the osmate-catalyzed Sharpless dihydroxylation of alkenes as model reaction for our investigations (Figure 1).

Conjugates of enzymes and poly (2-methyl-oxazoline) (PMOx), generated by coupling of the terminal amino group of the polymer and the amino groups of the enzyme via pyromellitic acid dianhydride, are soluble in organic media, e.g. chloroform.

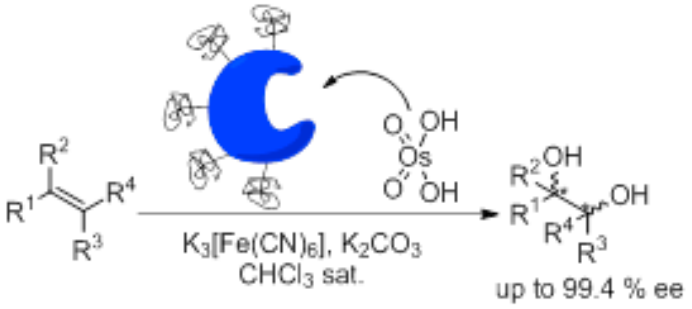

Figure 1: Sharpless dihydroxylation with polymer enzyme conjugates as ligand.

One great advantage of these organo-soluble PECs is that they can act as amphiphilic core-shell nanocontainers. Potassium osmate is not soluble in chloroform. After adding the salt to a PEC solution in this medium, it can only be dissolved by being complexed to a hydrophilic core, which is the protein part of the PEC. Thus, the osmate is forced into the chiral environment of the enzyme and thereby incorporated by dative anchoring.

Investigations of a number of different conjugates of PMOx-enzyme conjugates revealed that the enantioselctive control of the Sharpless dihydroxylation can be controlled by the nature of the enzyme even favoring S- and R-configuration. The greatest selectivity was found for the laccase-PEC.

Optimizing the reaction conditions with laccase (from *trametes vesicolor*) PECs strongly indicates that osmate is located in the active site of this enzyme by a copper to osmate exchange (Figure 2). Therefore copper was previously deliberately removed from laccase by dialysis of the PECs against an aqueous ethylenediaminetetraacetic acid (EDTA) solution.

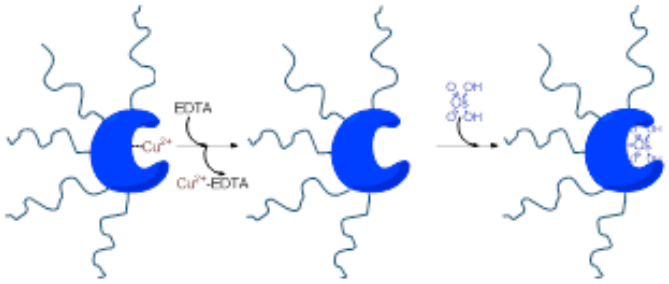

Figure 2: Scheme of the suggested copper type 1 to osmate exchange by treatment of the laccase-PEC with EDTA as Cu-scavenger.

It was shown that the resulting artificial metalloenzyme catalyzes the dihydroxylation of alkenes in chloroform and affords highly enantioselective product formation. Thereby product enantioselectivities up to 99.4 % *ee* were achieved, which even exceeds the classical Sharpless catalysts. Thus, we could transfer the concept of artificial metalloenzymes from water to organic solvents with even higher selectivity. Current work is dedicated to broaden the concept to other enyzmes and further reactions.

Publications:
S. Konieczny, M. Leurs, J. C. Tiller, Polymer Enzyme Conjugates as Chiral Ligands for Sharpless Dihydroxylation of Alkenes in Organic Solvents, ChemBioChem 2015, 16, 83 – 90.

Contact:
melanie.leurs@bci.tu-dortmund.de
joerg.tiller@tu-dortmund.de

Double Action Polyoxazolines for Dental Applications

Antimicrobial and Collagenase-inhibiting Polymer for caries prevention in dental materials

Christoph Fik, Stefan Konieczny, Jörg C. Tiller

Mechanical removal of caries infected tooth material is already inducing secondary caries, because the caries-causing cells are forced into the tubuli below the treated dentin. Eventually, the surviving bacteria will form caries below the dental filling. Even if the microbial cells are killed in the process, there is still the problem of the bacteria-related enzyme collagenase, which is still active causing degradation of the collagen fibers below the filling, which results in decreased adhesion of the filling. Thus, the optimal additive for a dental filling will be a compound that kills microbial cells, inhibits collagenase, and is bound to the surface of the dental filling for prolonged activity. The here developed telechelic polyoxazoline is a promising candidate for meeting these requirements.

Modern dental repair materials face the problem that the dentin below the composite fillings is actively decomposed by secondary caries and extracellular proteases such as MMP.

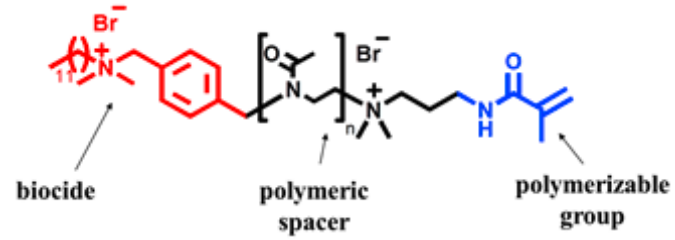

Figure 1. Chemical structure of DDA-X-PMOX-AMA

To address this problem, poly(2-methyloxazoline) (PMOx) with a biocidal and a polymerizable terminal was synthesized by cationic ring-opening polymerization of 2-methyloxazoline using a tailored antimicrobial initiator and a double bond-containing termination agent (structure see Fig. 1).

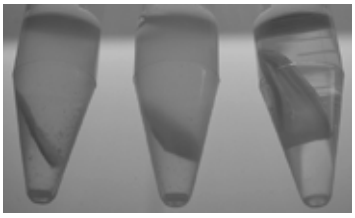

Figure 2. Photographs of eppendorf tubes containing cow tooth slices after 1 day of incubation in growth medium. The slices were infected with caries and treated with AdheSE® One F containing different concentrations of DDA-X-PMOx-AMA.

This polymer was explored as additive for a commercial dental adhesive. The additive rendered the adhesive contact-active antimicrobial against the caries related bacterium Streptococcus mutans at a concentration of 2.5 wt% and even constant washing with water for 101 days did not diminish this effect. Five wt.% of the additive in the adhesive allowed killing *S. mutans* cells in the tubuli of bovine dentin (see Fig. 2). No clouding, i.e. no bacterial growth, could be observed indicating successful killing.

Further, the additive fully inhibited bacterial collagenase at 0.5 wt% and significantly reduced activity of human recombinant collagenase MMP-9. Human MMPs naturally bound to dentin were inhibited by more than 96% in a medium containing 5 wt% of the additive One wt% of the polymer fully prevents degradation of cow tooth collagen for at least 48h (see Fig. 3b).

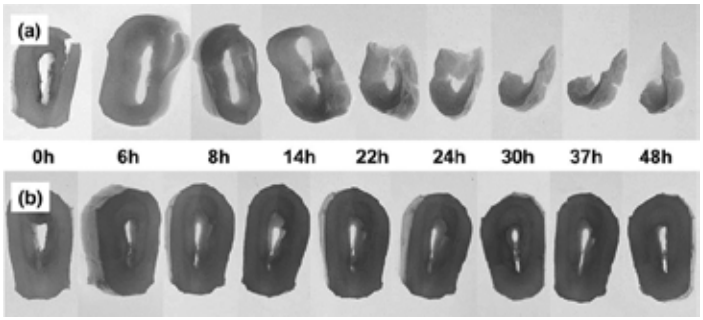

Figure 3. Photographs of decalcified cow dentine disks impregnated in citrate buffer with 1 mg collagenase. a) Non-treated disks. b) disks incubated with a 1.0 wt% DDA-X-PMOx-AMA/citrate solution for 1 h at room temperature and air dried.

In order to explore if the dental adhesive is still effective with the additive, its influence on the enamel and dentine bond strength of AdheSE® One F was measured. The macromer DDA-X-PMOx-AMA was added to AdheSE® One F (2.5 wt.%) and the respective shear bond strengths were determined for both formulations. In comparison to the reference, no significant decrease in both bond strengths was detected; the measured values were in a common range for corresponding dental adhesive compositions.

Contact:
joerg.tiller@tu-dortmund.de

Publikationen:
C. P. Fik, S. Konieczny, D. H. Pashley, C. J. Waschinski, R. S. Ladisch, U. Salz, T. Bock, J.C. Tiller

Telechelic Poly(2-oxazoline)s with a Biocidal and a Polymerizable Terminal as Collagenase Inhibiting Additive for Long-Term Active Antimicrobial Dental Materials Macromolecular Bioscience 14 (11), 1569-1579 (2014)

Shape-Memory Polypropylene

Robin Höher, Thomas Raidt, Frank Katzenberg, Jörg C. Tiller

Shape Memory Polymers (SMPs) are smart materials that switch shape at a certain trigger, e.g., temperature. Cross-linked polyethylene is the first shape memory polymer (SMP) known since 1960s and used in many applications such as shrink tubings. Interestingly, polypropylene (PP), a mass polymer with remarkable mechanical properties, could not be turned into a SMP, yet. This is due to the fact that PP cannot as easily be cross-linked as other polymers, which is the main prerequisite for obtaining a SMP that can fully recover its original shape. Here, we describe a new way of crosslinking PP, which renders the PP into a SMP with outstanding performance and interesting microstructure.

We chose to use maleic anhydrate (MA) for chemical modification of isotactical polypropylene prior to radical cross-linking. To this end, iPP was mixed with 2 wt. % dicumyl peroxide (DCP) and 4 wt. % maleic anhydride (MA) in a twin-screw extruder. Then the modified PP was cross-linked by adding 5 wt. % zinc oxide (ZnO), 2 wt. % glycidyl methacrylate (GMA) and 2 wt. % tetramethylthiuram disulfide (TMTD), further mixing, extruding, and curing in a heating press.

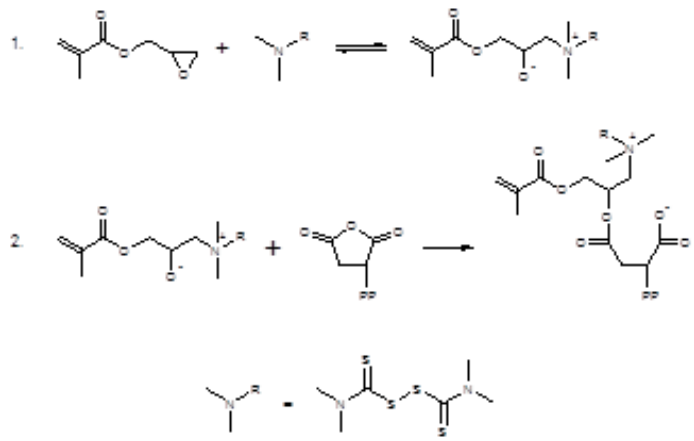

Figure 1: Assumed coupling reactions of GMA to the PP-g-MA.

The obtained PP-network exhibits excellent shape memory properties. After a first conditioning cycle it is capable to store fully recoverable strains of up to 680%. The average trigger temperature was determined as $T_{trig,x\text{-}iPP}$ = 158°C.

WAXS measurements of the programmed x-iPP revealed that not all crystals are oriented parallel but a significant amount of crystals is oriented at angles of 80° and 100° to the stretching direction (see Figure 1b).

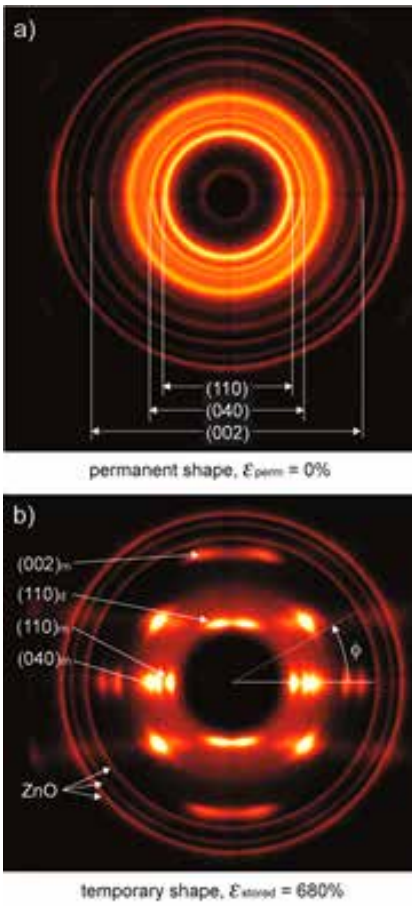

Figure 2: X-ray diffraction patterns of a) the permanent (εperm = 0%) and b) the programmed shape of x-iPP (εstored = 680%).

This can be explained by the literature known effect of iPP homoepitaxy, where “daughter” crystals grow onto the (010)-planes under 80° and 100° apart to the “mother” crystals, that are parallel oriented to the stretching direction during programming. Typically, the amount of mother crystals is larger than that of daughter crystals. Interestingly, here a higher fraction of daughter crystals compared to mother crystals was found.

Contact:
robin.hoeher@tu-dortmund.de
thomas.raidt@tu-dortmund.de
frank.katzenberg@tu-dortmund.de
joerg.tiller@tu-dortmund.de

Publications:
R. Hoeher, T. Raidt, F. Katzenberg, J. C. Tiller
Macromolecular Chemistry and Physics 36, 2015, 744-749

Defined Polymer Nanostructures for High Enzyme Activity

Revealing the origin of enzyme activation in APCNs in organic solvents

Ina Sittko, Jörg C. Tiller

Enzymes are natural catalysts with exceptionally high activity and selectivity in water. Although, they selectively catalyze reactions in organic solvents as well, their activity is several orders of magnitude lower in such media. Since most fine chemicals are not soluble in water, high enzyme activity is required for the practical use of biocatalysts in industrial syntheses. We have previously discovered that amphiphilic polymer conetworks (APCNs) activate entrapped enzyme in organic media. In this study, we have developed APCNs tailored to clarify the working mechanism of the biocatalytic materials. It was found that the defined nanostructure of APCNs is indeed the major factor for activation of entrapped enzymes.

The general concept of activation of enzymes in APCN is that the enzyme is located in the hydrophilic nanophase, while the substrate diffuses to the hydrophobic nanophase, is converted at the large interface under enzyme catalysis and the product diffuses out of the conetwork via the same nanophase. According to this concept, the best activity should be obtained in the APCN with two interconnected phases, which is typical for APCNs with some 50 % of both different polymer volume fractions. The enzyme activation should be solvent independent, if the activation is achieved by the large interface. So far, this has never been observed for all explored biocatalytic APCNs, most likely, because there are influencing parameter, such as swelling, that overlap the true activation effect.

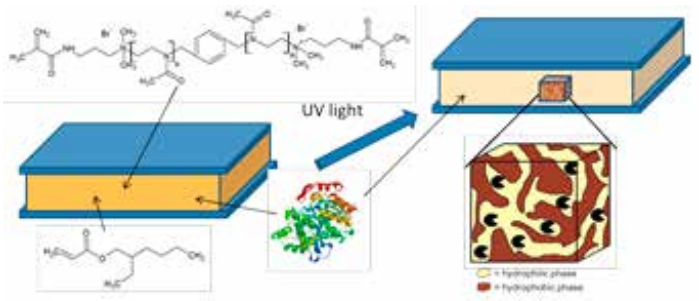

Figure 1. Sketch of the synthesis of APCNs with an entrapped enzyme.

In this study, we prepared two new APCNs, which allow entrapment of enzymes during preparation by copolymerization of n-butyl acrylate and 2-ethylhexyl acrylate, respectively, with telechelic methacrylamide terminated poly (2-methyl oxazoline) (PMOx). Both APCNs have a distinguished nanostructure shown by atomic force microscopy (see Fig. 2 on the example of PBuAc-l-PMOx). Their major advantage is that PBuAc-l-PMOx swells in toluene but not n-heptane, while the structurally close PEhAc-l-PMOx is swellable in both solvents. This gives us the opportunity to distinguish between swelling and structural effects on enzyme activity. The common lipase Cal B was entrapped in a series of the APCNs.

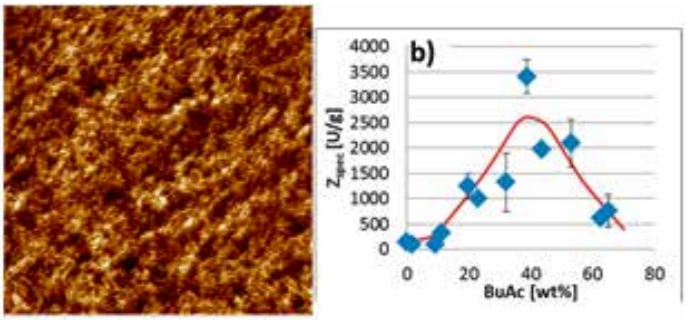

Figure 2. Left (a): Atomic force microscopy image of a PBuAc-l-PMOx APCN with approximately 50 vol% of each polymer phase, measured in phase modus. Right (b): Specific activity of entrapped lipase in PBuAc-l-PMOx of different compositions in toluene.

Lipase Cal B entrapped in the conetworks is most active at a composition that contains some 50 wt.% PMOx in all cases. Further, the maximal activation of Cal B with respect to the suspended powder is some 20-fold independent on the solvent as long as the APCN is swellable. This supports the proposed mechanism of enzyme activation in APCNs.

Although the activation of some 20-fold within the APCNs is exceeded by other supporting materials, the formation of particles out of the bioactive amphiphilic conetworks has been found to overcome diffusion limitation and greatly activates the entrapped enzymes compared to the here presented polymer films. Thus, we will strive to prepare the here developed APCN as particles in future work.

Contact:
Joerg.Tiller@tu-dortmund.de
Ina.Sittko@bci.tu-dortmund.de

Publications:
I. Sittko, K. Kremser, M. Roth, S. Kuehne, S. Stuhr, J. C. Tiller
Amphiphilic Polymer Conetworks With Defined Nanostructure and Tailored Swelling Behavior for Exploring the Activation of an Entrapped Lipase in Organic Solvents
Polymer 64, 122-129 (2015)

Toughening of artificial, shell-like composite materials using post polymerization process

Increasing material properties of urease-induced calcified hybrid materials by maximizing adhesion area between organic and inorganic phase

Nicolas Rauner, Lea Bünger, Stefanie Schuller and Jörg C. Tiller

Last year we introduced an innovative method to artificially produce shell-like $CaCO_3$ composite materials in large scale by intrinsic mineralization of water-swellable polymers. Unfortunately the mechanical properties of these artificial hybrid materials are not in the high range of the natural idol. By improving the process of urease-induced calcification and introducing a second polymerization step after calcification of the hydrogel the interface area of $CaCO_3$ and polymer phase could be increased. The consequence was a significantly higher toughness and an increased Young's modulus up to 3.5 GPa.

Artificial biomaterials have great potential in regenerative medicine and light-weight design, because of their high biocompatibility and good mechanical properties. Unfortunately the reproduction of the nanostructure, which is essential for their mechanical characteristics, was just successful in microscale. Urease-induced calcification of hydrogels is the first method that allows producing intrinsic calcified, nanostructured hybrid materials in a macroscopic scale at mild temperatures. Thereby urease is dissolved in an organic mixture of monomers like 2-hydroxy ethyl acrylate (HEA) or N,N-dimethyl acrylamide (DMA) and triethylene glycol dimethacrylate (TEG). After polymerization using UV-light the enzyme in the formed hydrogel is still active. Swollen in a solution of CaCl2 and urea, the embedded urease cleaves urea to ammonia and carbonate while latter leads to a selective CaCO3 crystal growth inside the polymeric hydrogel. The so grown composites show similarities to the natural structure nacre, but don't achieve its mechanical properties. With intent to improve the Young' modulus it was found that the pH value is changing during calcification process and has a direct influence to the nanostructure of the crystals. By stabilizing the pH using 0.1 M TRIS-buffer the content of CaCO3 was increased up to 95 wt%, which is the same as nacre.

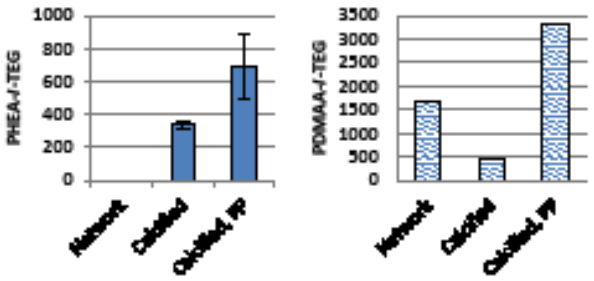

Figure 1: Young's moduli of different types of hydrogelsconetworks before and after calcification / post-polymerization (PP) steps.

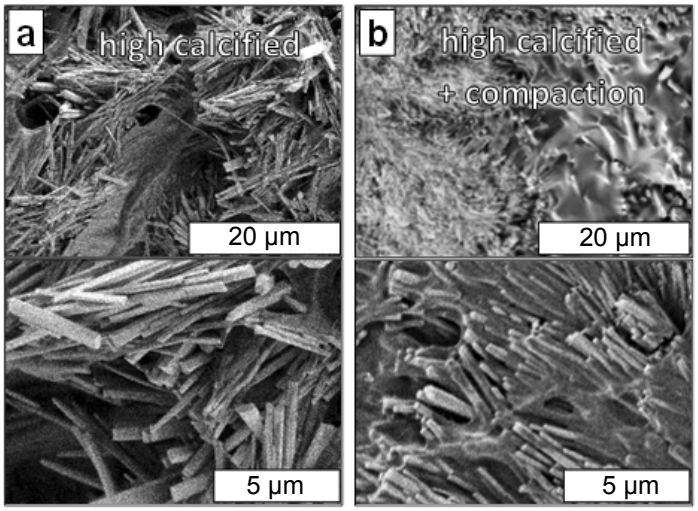

Figure 2: SEM images of (a) highly calcified HEA-*l*-TEG hydrogel and (b) the same network after an additional post polymerization step. The pictures beneath show magnified details of the images above.

The high inorganic content of the composites results in a change of mechanical properties dependent on the type of used network. Like shown in Figure 1 low-T_g-networks (HEA-*l*-TEG) reveal an increased Young's modulus due to the high $CaCO_3$ content (up to 330-times) compared to the bare conetwork. In contrast high-T_g-networks (DMA-*l*-TEG) show a loss of Young's modulus by calcification. An explanation might be the lack of adhesion between crystals and polymer matrix like shown in Figure 2a. The mechanical behavior of high calcified films is just dictated by crystal interlocking. Introducing a second post-polymerization (PP) step after calcification by swelling the hybrid material in a PHEA/PDMMA-*l*-TEG monomer solution and polymerize it increases the interface area between $CaCO_3$ and polymer (Figure 2b). The consequence is a significant rise in Young's modulus after this step that is up to 6-times higher than without PP and 50-times greater than that of the previously reported materials.

Publications:
N. Rauner, L.Buenger, S.Schuller, J.C. Tiller, Macromolecular Rapid Communication 32 (2), 224-230 (2015)
N. Rauner, M. Meuris, S. Dech, J. Godde and J.C. Tiller, Acta Biomaterialia 10 (9), 3942-3951 (2014)

Contact:
nicolas.rauner@udo.edu
joerg.tiller@udo.edu

Chemical Biotechnology (BT)

We Stick Together

Characterization of trophic autoaggregation

Karolin Schmutzler, Octavia Natascha Kracht, Andreas Schmid, Katja Bühler

The interesting biocatalyst Pseudomonas taiwanensis *VLB120 normally grows either planktonically in dispersed single cells or in multicellular communities attached to surfaces and embedded in an extracellular matrix, referred to as biofilms. Now, we discovered additionally the formation of clearly visible cell aggregates in liquid culture by several Pseudomonas taiwanensis VLB120 mutants. Remarkably, the autoaggregation of the mutants was induced by the nature of the supplied carbon and energy source. A comprehensive characterization of the aggregation behavior revealed several interesting facts about the physiology of the respective mutants.*

By investigating the growth behavior of several *Pseudomonas taiwanensis* VLB120 mutants, we found that the autoaggregative behavior only occurred when growing on defined carbohydrates as sole carbon and energy source while the wild type grew in suspended cells under all condition (Fig. 1).

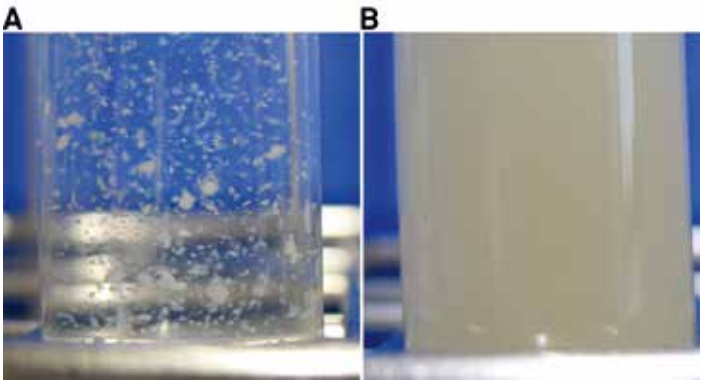

Figure 1: Culture of an autoaggregative mutant (A) in comparison to the dispersed growth of the parent strain *Pseudomonas taiwanensis* VLB120.

Furthermore, we observed that all mutants developed wrinkled colonies when plated on solid agar plates (Fig. 2) that were remarkably different from the normal smooth colony morphology of the parent strain.

Figure 2: Wrinkled colony morphology of an autoaggregative mutant on a congo red agar plate.

Additionally, we revealed that irrespective of the mutation, the second messenger c-di-GMP, which is known to be a central regulator of the transition between biofilm formation and motility, was involved in autoaggregation in all mutants.

Investigation of the outer layer of the cell membrane showed that the mutants exhibited an altered lipopolysaccharide (LPS) composition compared to the wild type. Further, we found that the altered LPS composition caused a significantly enhanced cell surface hydrophobicity of the mutant strains which was quantified for instance by contact angle measurements as shown in Fig. 3.

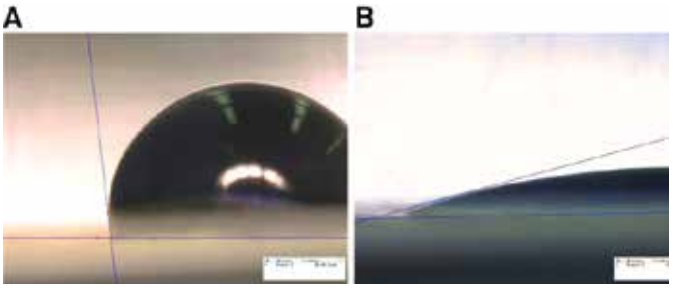

Figure 3: Contact angle measurement of a water drop with a layer of the mutant cells on a cellulose filter indicating a hydrophobic cell surface (A) in comparison to hydrophilic cells of the wild type (B).

Thus, these results supported the idea that the autoaggregation probably originated from hydrophobic interactions of the cells amongst each other.

The appealing characteristics of the aggregating mutants may also be very beneficial for future biotechnological applications of the strains for instance in bioconversions of hydrophobic substrates.

Publications:
Schmutzler K., Kracht O., Schmid A., Bühler K. 2015,Applied Microbiologa and Biotechnology accepted

Schmutzler K., Schmid A., Bühler K. 2015, Applied Microbiology and Biotechnology, 2015, 99, 6035-6047

Contact:
karolin.schmutzler@bci.tu-dortmund.de
andreas.schmid@ufz.de
katja.buehler@ufz.de

Mixed-culture resting cell fermentation

Biotechnological (*S*)-perillyl alcohol production

Christian Willrodt, Anna Hoschek, Bruno Bühler, Andreas Schmid, Mattijs K. Julsing

Oxygenated monoterpenoids constitute a group of natural products, which is of interest for chemical and pharmaceutical industry. In many cases isolation of monoterpenoids is hampered by the low abundance of these compounds in their natural sources, like plants. Biotechnological production from renewable substrates using recombinant microbial host organisms can serve as an alternative for traditional isolation or chemical synthesis approaches.

Many interesting natural products have properties, which do not directly match to biotechnological production. Were microbial metabolites are in general hydrophilic, natural products are often of hydrophobic, volatile, or even toxic to host organisms. In the past, we successfully developed a setup for the fermentative production of the carbon skeleton limonene in *E. coli* applying an organic:aqueous two-liquid phase system. Limonene toxicity and evaporation could be circumvented by in-situ extraction in the organic phase. Also, the biotransformation of limonene into (*S*)-perillyl alcohol has shown to be an efficient process using *E. coli* containing a cytochrome P450 monooxygenase (CYP450) from *Mycobacterium* sp. strain HXN-1500.

Here, we found that combining the oxygenation catalyzed by the CYP450 with the fermentative production of limonene in one recombinant *E. coli* strain, was not so straight-forward as the introduction of the CYP-genes in the limonene producing strains. Therefore, strategies were investigated in order to develop a process setup for fermentative (*S*)-perillyl alcohol production.

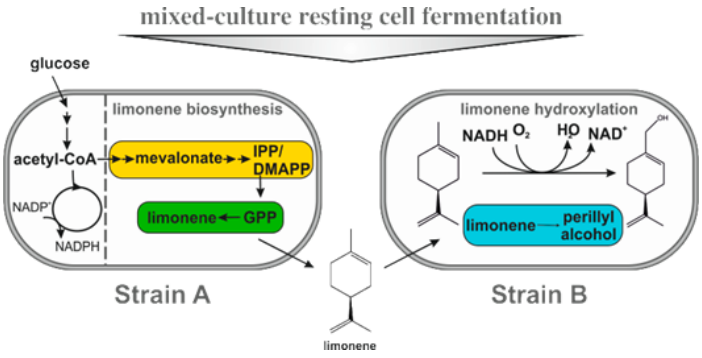

Figure 1: overview for the production of (*S*)-perillyl alcohol by the mixed-culture resting cell fermentation.

First, we tried to tackle the intrinsic activities and stabilities of the CYP450 by the construction of all downstream genes on one plasmid, which enabled the functional expression of all genes at the same time.

In addition, an artificial fusion of the monooxygenase and terpene cyclase was designed to bring the two enzymes in spatial proximity. Finally, an alternative monooxygenase CymA was investigated. The three strategies of genetic engineering did result in the production of (*S*)-perillyl alcohol, but titers remained low, probably caused by fast extraction of limonene in the organic phase or evaporation.

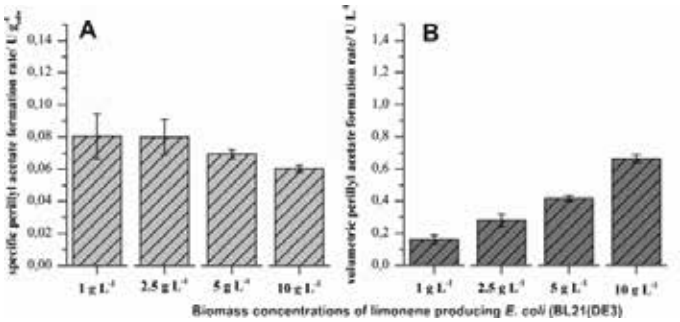

Figure 2: Specific (A) and volumetric (B) product formation rates for the production of oxygenated monoterpenoids by mixed-culture resting cell fermentation using varying cell densities (gCDW L-1) of limonene producing *E. coli* cells and a fixed amount of 1 gCDW L-1 CYP450 containing cells. (CDW: cell dry weight).

We therefore introduced the concept of mixed-culture resting cell fermentation (Fig.1). Both, a limonene producing strain and a strain containing the monooxygenase components were grown separately and combined as resting, but metabolically active, cells in a defined ration. Mixed-culture resting cell fermentation resulted in the effective production of oxygenated monoterpenoids (Fig.2).

This modular approach is complementary to and can be combined with metabolic engineering strategies. It provides a platform to access the synthesis of a variety of oxygenated monoterpenoids Furthermore, mixed-culture resting cell fermentations may serve as general tools to perform cascade reactions involving intermediates and products with challenging properties, such as high volatility and low solubility.

Contact:
mattijs.julsing@bci.tu-dortmund.de
bruno.buehler@bci.tu-dortmund.de
christian.willrodt@ufz.de
andreas.schmid@ufz.de

Publications:
Willrodt C., David C., Cornelissen S., Bühler B., Julsing M.K., Schmid A. Biotechnology Journal 2014, 9, 1000–1012

Willrodt C., Hoschek A., Bühler B., Schmid A., Julsing M.K. Biotechnology & Bioengineering 2015, 112, 1735-1750

Biochemical Engineering (BVT)

A mathematical model for enzyme-catalyzed esterification

Development of an optimized kinetic model considering different reaction conditions

Dana Boettcher, Waldemar Krieger, Rolf Wichmann

As a reference system the synthesis of the fruit ester isoamyl acetate (IAAc) is investigated by using an immobilized lipase. IAAc is an important flavor and fragrance compound, which is widely used in the food, beverage, and cosmetic industry. The kinetic mechanism of enzyme-catalyzed esterification is usually described by a Ping-Pong Bi-Bi mechanism, which provides good results at reproducing experimental data. But there are still mathematical models missing, which are also able to predict the product concentration during the reaction. Therefore in this work the reaction kinetics for the synthesis from isoamyl alcohol (IAA) and acetic anhydride (AAnh) in solvent-free media was modeled, taking the influence of temperature T (between 35°C and 90°C) and substrate ratios SR (IAA: AAnh from 3:1 to 7:1) into account. The results of validation experiments show that differences between theoretical and experimental data are less than 7 %.

The main reaction between IAAc (Q) and AAnh (A) and the secondary reaction between the produced acetic acid (AAc) and IAA (B) cannot be catalyzed at once, thus they are treated as competitive reactions. The inhibiting effect of AAc (C,P) is also included in the model, but a significant inhibition by AAnh is not observed. Furthermore, no reverse reactions are included, except the inhibition reactions, due to the experimental data. Additionally the uncatalyzed side reaction between the AAnh and the produced water (R) has to be considered in the rate equation for acetic acid. In order to incorporate the temperature dependency of the esterification, the positive effect is implemented in the maximum velocity for the enzyme (E) activity according to the Arrhenius equation, as well as for the uncatalyzed side reaction. The negative effect influences the catalytic activity of the enzyme itself, but experiments reveal that it is suitable to consider the enzyme deactivation in the rate equations by using a dependency of the AAc concentration. This all ends up in an equation for the reaction rate for the product IAAc:

$$r_Q = \frac{r_{1,1}\exp\left(\frac{-E_{a,1}}{RT}\right)AB + r_{1,2}\exp\left(\frac{-E_{a,2}}{RT}\right)\frac{k_{cat,BC}}{k_{cat}}BC}{K_{mA}AB + K_{mB}\frac{k_{cat}}{k_{cat}}C\left(1+\frac{C}{K_{iC}}\right) + AB + \frac{k_{cat}}{k_{cat}}BC}[E]_0\exp\left(-k_c\frac{C}{C_{max}}t\right)$$

This equation is validated with experiments conducted at different T and SR (ref. fig. 1), which were not used for the adjustment of the kinetic constants.

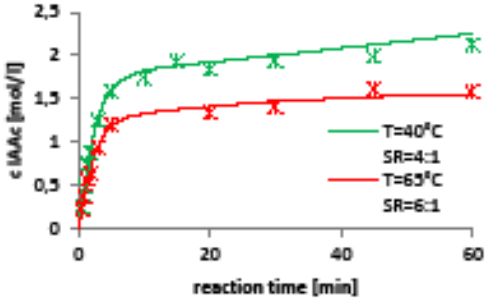

Figure 1: Comparison between modeled (lines) and measured (points) values for two validation experiments.

Although the experiments conducted to gain the data for fitting parameters lasted 1 hour, the model is also valid to predict the concentrations for a longer period of time, until the acyl donor AAnh as well as the produced AAc in a subsequent reaction are completely exhausted (ref. fig. 2).

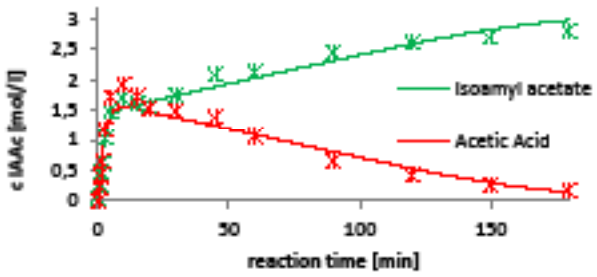

Figure 2: Comparison between modeled (lines) and measured (points) values until the substrates are exhausted

Additionally it is feasible to predict the product concentration achieved with different amount of immobilized enzyme (ref. fig. 3).

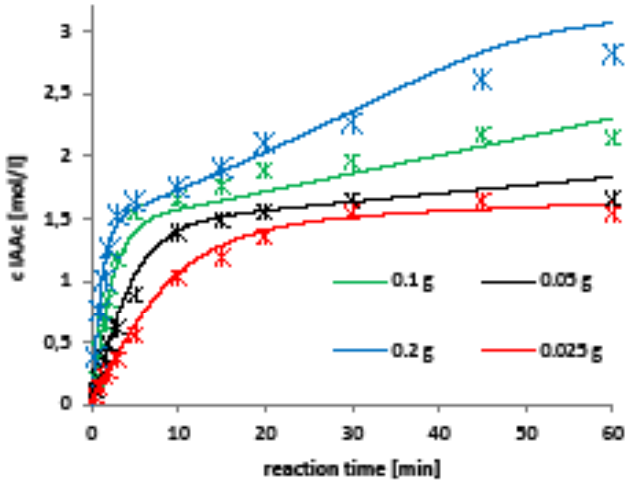

Figure 3: Comparison between modeled (lines) and measured (points) values for different immobilized enzyme amounts.

Contact:
dana.boettcher@tu-dortmund.de
waldemar.krieger@tu-dortmund.de
rolf.wichmann@tu-dortmund.de

Production of Fusicoccadiene by Saccharomyces cerevisiae

Precursor of several potential anti-cancer drugs

Lisa Halka, Michaela Freder, Rolf Wichmann

Fusicocca-2,10(14)-diene (FCdiene) has a potential in the pharmaceutical industry as a precursor of several potential anti-cancer drugs, for example cotylenin A or fusicoccin A. Naturally FCdiene is produced only at low titers in wild strains of certain phytopathogenic and filamentous fungi which cannot be cultivated in laboratory. Therefore a heterologous Saccharomyces cerevisiae is used for the production of FCdiene. For an industrial economic production of FCdiene the required fermentation and downstream technology has to be developed.

FCdiene is a di-terpene and consists of a 5-8-5 tricyclic carbon skeleton (Fig.1) which assigns the FCdiene to the group of the fusicoccanes. It completely consists of carbon and hydrogen atoms, what leads this molecule to a very hydrophobic character. On the one hand this leads to an ambitious fermentation strategy using a hydrophilic medium. But on the other hand the hydrophobicity of FCdiene can be exploited for the separation step by either adsorption or liquid-liquid extraction or even for an integrated product separation step.

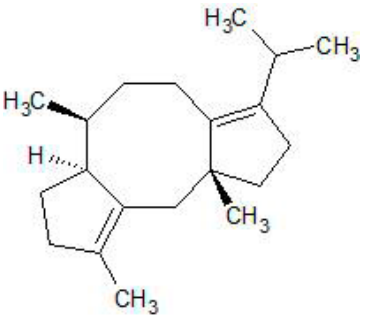

Figure 1: Chemical structure of FCdiene

Fermentations of a genetically modified Saccharomyces cerevisiae strain (kindly provided by the group of Prof. F. Schulz, Ruhr University Bochum) using SD-medium and glucose as substrate showed in the beginning a product titer of about 35 mg/L FCdiene after 48 h.

Previous experiments have shown, that the pH could have an influence on the product structure and on the progress of the process. This is tested by using a start-pH of 6.9, buffering the medium at pH 6.9 and adding $CaCO_3$ to the buffered medium. Only the $CaCO_3$ could prevent a drop of pH. In the buffered medium the pH drops to 5 and when starting at pH 6.9 it drops to 2.9 in the unbuffered medium, which nearly is the pH of 2.5 of the reference. The corresponding product yields at the time of the maximum product concentration (Fig. 2, top) show that higher pHs inhibit the FCdiene production, although the pH falls nearly to the same value. The maximal product yield is more than 2 times lower than for the reference.

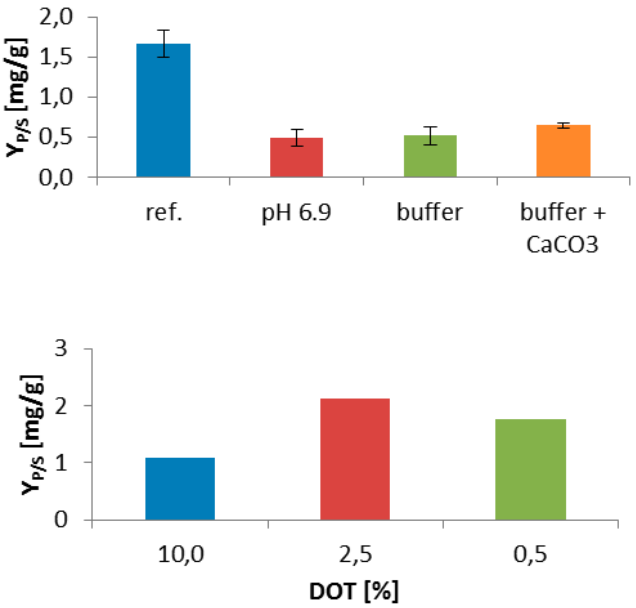

Figure 2: Substrate specific yields changing the pH (top) and changing the DOT (bottom)

Previous experiments show as well that the DOT (dissolved oxygen tension) has an influence on the production process of FCdiene in Saccharomyces cerevisiea. The DOT is changed at 2 L scale from 10 %, to 2.5 % and 0.5 %. The results in figure 2 (bottom) show that the best production of FCdiene could be achieved at a DOT of 2.5 %. Regulation of a DOT at around 0.5 % is not easy to maintain so that the total volume of air was nearly the same as for a DOT of 2.5 % and no increase in yield was reached.

Contact:
lisa.halka@tu-dortmund.de
rolf.wichmann@tu-dortmund.de

Chemical Reaction Engineering (CVT)

Liquid-liquid mass transfer in micro-channels

Wall film participation for mass transfer in liquid-liquid slug flows

Florian Kaske, Stefanie Dick, Linda Arsenjuk, David W. Agar

Extraction processes in micro-channels are particularly interesting for expensive materials due to their excellent mass transfer rates and low liquid hold-ups. In liquid-liquid slug flow mass transfer is enhanced by internal vortex circulation. Another special feature of this flow regime is the formation of a wall film of the continuous phase around the dispersed slugs of the non-wetting phase. The decisive behaviour of this wall film and its contribution to the overall mass transfer process is very complex, but has nevertheless been elucidated in this work.

Liquid-liquid slug flow is a flow regime in micro-channels which allows well-regulated and scalable residence times by virtue of the well-defined flow structure. Furthermore, the overall mass transfer is very rapid due to the small distances and high interfacial areas. In segmented flows it is further increased by internal circulations inside the slugs. These so-called Taylor-vortices, lead to positive interactions between the diffusive and convective mass transfer. Therefore, the mass transfer rates achievable in microstructures are at least one order of magnitude higher than those in conventional macro-reactors.

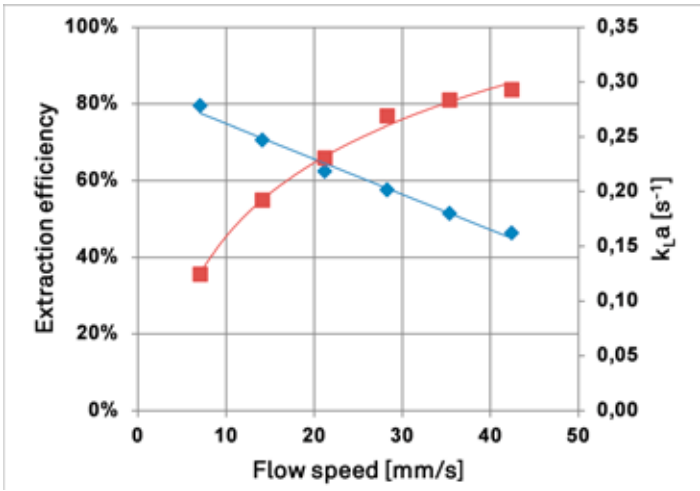

Figure 1: Measured extraction efficiencies and specific mass transfer coefficients for the system Water-Acetic Acid-Kerosene (L_{Slug}=3 mm, capillary diameter 1 mm, length of capillary 90 mm))

In Figure 1 the extraction efficiency determined for the system Water-Acetic Acid-Kerosene is depicted. It is apparent that the extraction efficiency decreases with increasing flow rate. On the other hand, the mass transfer coefficient kL·a [s^{-1}] rises due to the intensified internal circulations at higher flow rates, but the influence of the residence time dominates.

In general, the overall mass transfer between the dispersed and continuous phase is comprised of three different contri-

Contact:
florian.kaske@bci.tu-dortmund.de
david.agar@bci.tu-dortmund.de

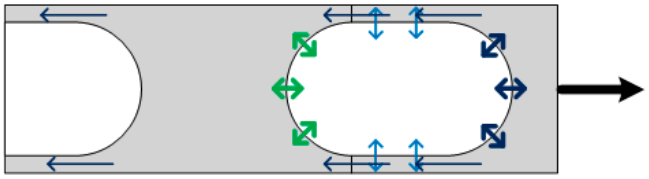

Figure 2: Visualisation of the three different mass transfer processes:

Front cap to continuous phase,
Rear cap to continuous phase
Dispersed slug to wall film

While the mass transfer between the caps of the dispersed slug and the continuous phase has already been considered, the participation of the wall film in the mass transfer is still unclear. Thus, to clarify wall film behaviour an experimental set-up with fluorescence microscopy was devised. A special feature of the experimental set-up is that the wall film is formed at a well-defined position due to a change in the wall material. From this point on, the back-mixing in the continuous phase over the wall film has been investigated for various two-phase systems.

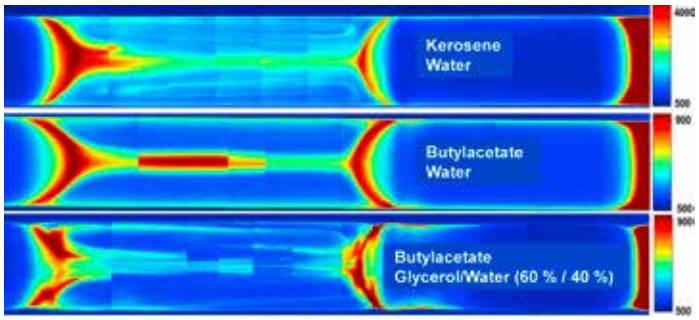

Figure 3: Degree of back-mixing of the tracer Fluorescein for the three investigated two-phase systems (flow direction from left to right, flow rate u=41.4 mm s^{-1})

From Figure 3 it can be appreciated that a fraction of the fluorescent tracer is transferred over the wall film to the following slugs of the continuous phase. Most of the wall film is then recirculated in front of the following slug. The experiments carried out indicate that the wall film participates in the mass transfer and that it is also renewed by the following slug of the continuous phase. The exact amount of renewal depends on factors like flow rate, slug shape and the physical properties of the two-phase systems and will be analysed in more detail in future work.

Suspension Catalysis using liquid-liquid-segment flow in micro-channels

A novel approach to heterogeneous catalysis in micro-reactors

Franziska Horbach, Frederik Scheiff, David W. Agar

Suspension catalysis overcomes the shortcomings of alternative techniques for implementing heterogeneous catalysis in micro-reactors. By using liquid-liquid segmented flow in micro-channel one can ensure both an adequate suspension of the catalyst to avoid blockages and good accessibility of the catalyst for the reaction medium. Since particle wettability rather than particle size is used for catalyst recovery, very small particles which are less susceptible to sedimentation and offer excellent mass transfer may be employed. A detailed understanding of the biphasic slug flow hydrodynamics is a prerequisite for achieving the good suspension and mass transfer characteristics sought. On the basis of this knowledge further effective process intensification measures have been devised.

Catalysis is usually the key to successful chemical conversion and solid heterogeneous catalysts are generally preferred due to their facile separation from the reaction medium, by filtration or sedimentation for instance. Catalyst recovery by such means thus often imposes a lower limit on the particle sizes, which should be as small as possible to avoid mass transfer limitations. Using catalyst wettability for separation purposes can circumvent these conflicting factors.

The so-called slug flow, a segmented flow of two im-miscible liquids in microcapillaries, offers advantages such as precisely defined residence times and an en-hanced mass transfer within and between the two phases. The latter is governed by Taylor-like vortices, which promote the interplay of convective and diffu-sive transport in each slug. However, these effects have not yet been exploited with heterogeneous catalysis. Instead, heterogeneous reaction concepts in microreactors have been restricted to either micro-fixed-beds or catalytically coated wall reactors. Nevertheless, suspension catalysis can provide clear benefits in terms of catalyst accessibility for the reactants and its facile recovery by simple liquid-liquid separation.

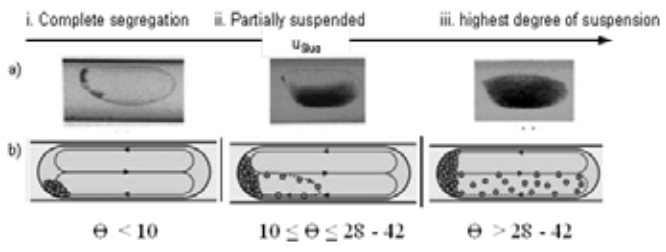

Figure 1: Segregation of catalyst particle suspension as a function of the Shields-Parameter (θ = Drag:Gravity) with increasing velocity

The capillary diameters typically employed lie between 1 and 2 mm, whilst the mostly hydrophilic catalyst support particles used are in the size range of 1-100 µm at concentrations between 0.5 and 20 wt.%.

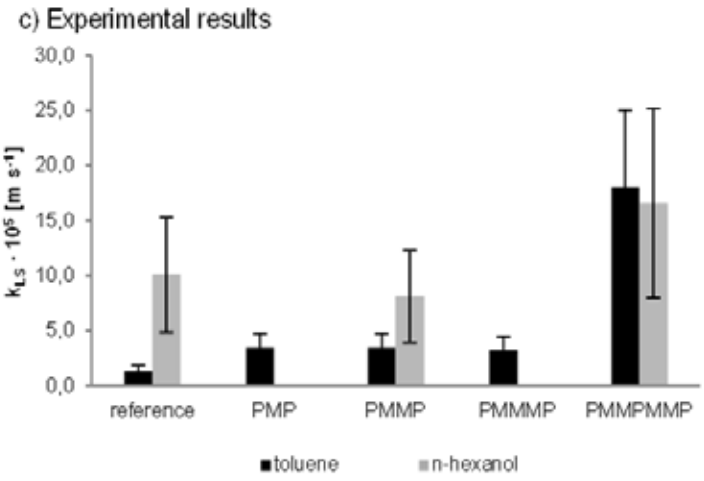

Figure 2: Mass transfer coefficients obtained with (multiple) alternating hydrophobic(P)-hydrophilic(M) wall materials

The last technique proved the most effective. The values illustrated in figure 2 indicate that mass transfer coefficients of a similar magnitude to those in intensively stirred reactor can be attained. In addition, it proved possible to treat the catalyst particles with silanisation to render them hydrophobic rather than hydrophilic, providing a useful extra degree of freedom in the choice of reaction medium, catalyst carrier liquid and wall material.

Publications:
A.-K. Liedtke, F. Scheiff, F. Bornette, R. Philippe, D.W. Agar, C. de Bellefon „Liquid–Solid Mass Transfer for Microchannel Suspension Catalysis in Gas–Liquid and Liquid–Liquid Segmented Flow" Ind. Engng. Chem. Res., DOI: 10.1021/ie504523y,17.04.2015

MicroDetec

A novel non-invasive measurement method for multi-parameter detection in microfluidic devices

Linda Arsenjuk, Nicolai Antweiler, Joachim Franzke, David W. Agar

The implementation of multi-phase reactions in micro-devices represents a technique for process intensification. Efficient mass and heat transfer, resulting from large surface-to-volume ratios, open up operating windows beyond the limits of conventional processes, while small volumes render the reactors safer and easier to control. To reap these advantages on an industrial scale, an affordable and robust process monitoring method is required. With MicroDetec a novel non-invasive measurement method was developed, which comprises a single simple and cheap set-up, and is applicable to a whole variety of measuring tasks.

Micro-reactors have become one of the focal points of research in the field of process intensification. Enhanced heat and mass transfer combined with low system inertia permit precise process control to raise conversions and selectivities. To exploit these benefits for process operation, suitable process monitoring systems must be developed for parallelisation purposes.

Conventional sensor concepts are often not applicable at the micro-scale or are expensive. The continuous operating mode and sensitive flow conditions in micro-reactors additionally call for measurements which are non-invasive and yield digital signals.

The novel MicroDetec sensor concept developed at the Chair of Chemical Reaction Engineering enables facile non-invasive on-line monitoring of chemical and physical process variables in micro-channels.

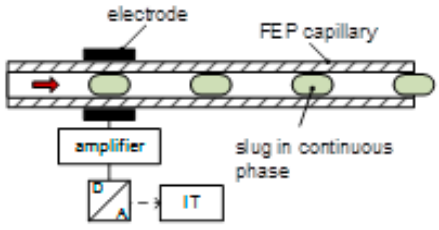

Figure 1: Schematic set-up of MicroDetec measurement device

We have found that for segmented flow in non-conductive micro-channels, the phases acquire unequal volume charge density as a result of triboelectric effects. This generates an electric field, which travels along the channel with the phases. Thus, a point in the vicinity of the channel will experience a continuously varying electric field, which can be captured to characterise the both the flow and other parameters.

The measuring principle makes use of this effect by utilising an electrode at the outer wall of the micro-channel to detect the small current induced by the change of electric field (Figure 1). The current is subsequently converted to a voltage and amplified, giving a signal which can then be digitised through conventional data acquisition systems. After digitisation, the signal can be mathematically operated upon with the help of software to estimate the variables of interest based on previously calibrated data.

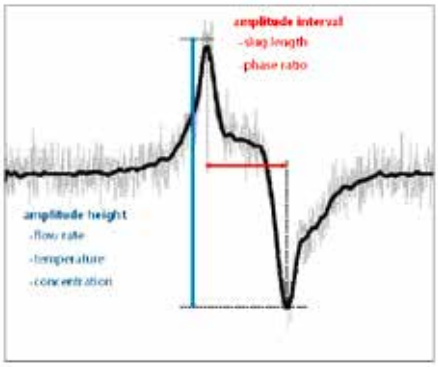

A slug passing by the electrode generates a voltage signal characterised by a positive and negative amplitude, as displayed in Figure 2. The height of and interval between the peaks provide information on physical and chemical process variables, such as flow characteristics, temperature and chemical composition.

The measuring principle is applicable to both, gas / liquid and liquid / liquid systems. Furthermore, it can be applied in a generalised ‘Lab in a Slug’ microanalytical sensor concept, where a slug, chemically tailored to the particular measuring task, is utilised as a measurement probe.

This unlocks a whole gamut of further application fields in non-invasive sensor technology and analytics appropriate for microfluidics, which will be the objective of future research.

Publications:
N. Antweiler, J. Franzke, G. Jestel, D.W. Agar
“Verfahren und Vorrichtung zur nichtinvasiven Bestimmung von Prozessparametern bei Mehrphasenströmungen” Patent pending, application filed 31.03.2014

Contact:
linda.arsenjuk@bci.tu-dortmund.de
david.agar@bci.tu-dortmund.de

Process Dynamics and Operations (DYN)

Definition and Visualization of Resource Efficiency Indicators for Chemical Production Processes

Fast perception of important information

Marc Kalliski, Daniel Krahé, Benedikt Beisheim[1], Stefan Krämer[1], Sebastian Engell
[1]INEOS Köln GmbH, Alte Straße 201, 50769 Köln

Operational decisions in the day-to-day business of chemical production processes can have a significant impact on the energy and material efficiency. This is often not transparent to operators due to complex interactions for highly integrated plants and the lack of standardized and systematic evaluation methods that capture the current resource efficiency. We propose to use real-time resource efficiency indicators (REI) to monitor the energy and material efficiency of chemical production plants in real-time and subsequently to use them in decision support for operating staff [1]. Trade-offs between energy efficiency, material efficiency and competing plant sections result in a multi-dimensional optimization problem that must be efficiently visualized for easy perception by operators and managers.

The material and energy efficiency of chemical production processes is strongly influenced by the operational decisions made during the daily production. The complexity and high degree of integration of the considered systems causes interrelations imposed by stoichiometry, heat integration and recycle streams to be opaque to the operator. For instance a locally optimized unit in plant A can cause a high energy demand in plant B due to heat integration and can subsequently result in a sub-optimal state of the overall production site (cf. fig. 1).

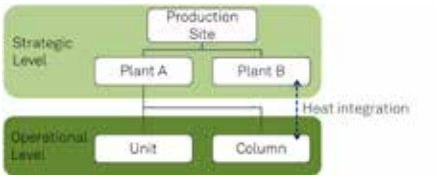

Figure 1: Hierarchical structure of Resource efficiency indicators

In our work we have established a structured methodology based on resource efficiency indicators (REI) to monitor the multi-dimensional resource efficiency in real-time and developed a visualization tool that enables operators and plant managers to identify inefficient operational states and conduct a root cause analysis to steer the plant towards improved resource efficiency.

The REI are based on a gate-to-gate approach with an integrated energy and material flow analysis within the system boundaries. In a first step the resource efficiency is measured on the operational level for all relevant sub-units with high granularity as resource and product specific indicators that are normalized by the theoretical or historical optimal value. Indicators on the strategic level are calculated by vertical aggregation to capture the overall resource efficiency. Furthermore, they are defined independent of external economic influences to show competing aspects of resource efficiency and the economic performance. This multi-criterial optimization problem is presented to the operator in the form of a dashboard enabling him to make informed decisions under the constraints posed by the market and management strategies (e.g. green production strategy).

Efficient dashboard concepts for multi-dimensional REI information require visualization elements that are best suited to highlight the intended relations and are easily comprehensible with little effort for interpretation. To exceed the possibilities of classical two- or three-dimensional representations, the use of additional attributes like color, orientation, size and a smart combination of specialized visualization elements are combined to dashboard solutions that reflect the contributions to the overall resource efficiency separately. Fig. 2 shows a clean dashboard developed for an acrylonitrile plant operated by INEOS Cologne including a control panel for the navigation through the plant hierarchy with built-in efficiency indicator bars for three plant sections indicating the overall efficiency (left). Upon user selection historical trends for the selected sub-section- and resource-specific REI are displayed as aggregated tiles (right). The current value and trend is shown by the color and orientation of the associated arrows next to the latest tile.

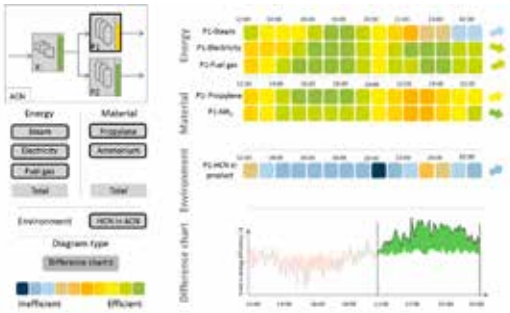

Figure 2: Dashboard for acrylonitrile plant operated by INEOS Cologne

For the example shown in fig. 2, the user can identify a deficiency in the plant section P1 that is caused by the inefficient use of steam and an elevated side product concentration in the product stream. Moreover, the plant operator can now navigate down the plant hierarchy of P1 to investigate further in combination with a variety of different diagrams accessible by a drop down menu (bottom-left).

Publications:
[1] M. Kalliski, D. Krahé, B. Beisheim, S. Krämer, S. Engell, Computer Aided Chemical Engineering, Vol 37, 1949-1954, 2015

Contact:
marc.kalliski@bci.tu-dortmund.de
sebastian.engell@bci.tu-dortmund.de

Real-time Optimization by Modifier Adaptation Based Upon Quadratic Approximation

Weihua Gao, Simon Wenzel, Sebastian Engell

Companies in the process industries face intense pressure to improve their production efficiency, while maintaining product quality and process safety. One means to achieve this goal is Real-time Optimization (RTO). The term means a periodic model-based steady-state optimization of the operating point of a unit or a production complex. Real-time optimization employs a process model which inevitably is inaccurate. In our work, we augment the model by a data-based component that represents the observed behaviour of the plant. This is done by using ideas from derivative-free optimization (DFO).

As a model-based optimization scheme, the success of RTO depends strongly on the quality of the model which is used in the optimization. The effort required for building and maintaining the model is the bottleneck in the deployment of RTO solutions, and even when sophisticated models are used, they will never exactly represent the real process. It is therefore highly desirable to combine the use of models and of the data which is collected during the operation of the plant in order to obtain a real-time optimization scheme that drives the plant to its optimal operation without having to represent each and every phenomenon in the plant accurately in the model.

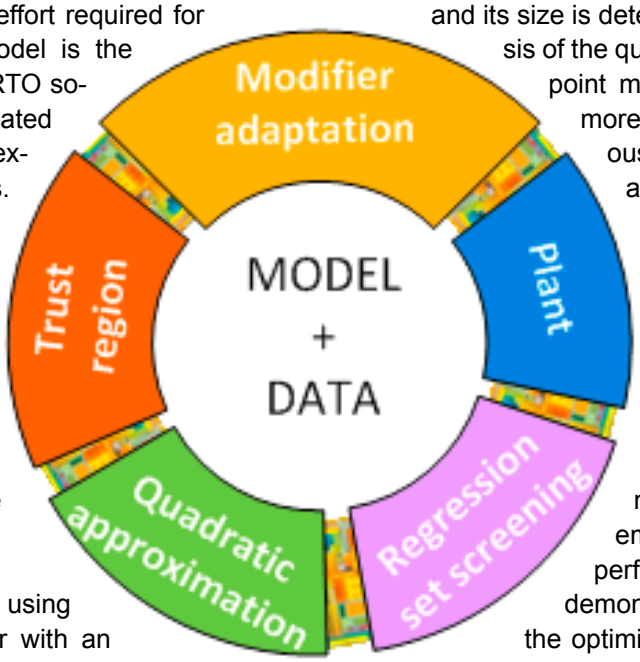

We propose a new scheme for using the collected plant data together with an inaccurate model in a way that assures that the iterative optimization converges to the optimum of the real plant. The new scheme combines the quadratic approximation that is used in derivative-free optimization with the iterative gradient-modification approach and integrates recent advances in both areas. The collected plant data is first screened, according to the distribution and the distance from the current operating point, to choose a so-called regression set. Quadratic approximations of the cost function and of the constraints are then constructed based on the collected data, and the gradients of the cost function and of the constraints with respect to the manipulated variables are computed from these approximate models. Compared with the finite-difference calculation of the process gradients that was used before, the quadratic approximation reduces the influence of the measurement noise. A trust-region for the next move of the process inputs is introduced and its size is determined from a covariance analysis of the quadratic regression set. Large set-point moves along a direction in which more data has been collected previously are permitted which leads to a fast rate of convergence. On the other hand side, moves along a direction in which the plant has not yet been probed much are bounded to avoid an inefficient deterioration of the plant performance. The next set-point move is then determined by modifier-adapted optimization which means to augment the model by empirical gradient information. The performance of the new scheme is demonstrated by simulation studies for the optimization of the Otto-Williams reactor in the presence of plant-model mismatch and measurement errors. One iteration of the optimizer is illustrated in the figure below showing the regression set, the quadratic approximation of the objective, the trust region, and the modifier-adapted optimization result.

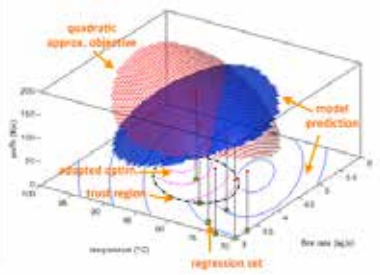

The research leading to these results was funded by the ERC Advanced Investigator Grant MOBOCON under the grant agreement No. 291458.

Contact:
weihua.gao@bci.tu-dortmund.de

Publications:

W. Gao, S. Wenzel, S. Engell. A Reliable Modifier-Adaptation Strategy for Real-Time Optimization. Submitted to Computers and Chemical Engineering

W. Gao, S. Wenzel, S. Engell. Comparison of Modifier Adaptation Schemes in Real-Time Optimization. In Proceedings of ADCHEM, Whistler, 2015

W. Gao, S. Wenzel, S. Engell. Modifier Adaptation with Quadratic Approximation in Iterative Optimizing Control. In Proceedings of for Euro-pean Control Conference, Linz, 2015.

Solids Process Engineering (FSV)

CFD Wet Scrubber Simulation

Predicting the Particle Collection Efficiency in a Venturi Scrubber

Damian Pieloth, Gerhard Schaldach, Peter Walzel

Venturi scrubbers are widely used in industrial processes for removing particles from gas streams. They are simple to build, robust in operation, especially when hot gas streams have to be cleaned or when sticky particles have to be removed from flue gas. Also, they are even capable of removing submicron particles efficiently from gas streams. Motivated by previous work, we used our own model of particle capture by droplets and the model of droplet breakup by Schmehl for CFD-simulations of venturi scrubbers. Our CFD simulations were also validated with experimental data obtained by Haller.

The CFD simulation of venturi scrubbers must comprise different physical effects: the disintegration of the scrubbing liquid into droplets, the collection of dust particles from the flue gas by the scrubbing liquid and the motion of a dense droplet assemble within a gas stream. Motivated by a successful CFD simulation of rotary scrubbers and spraying towers, we carried out the CFD simulation of venturi scrubbers by including the previous work a droplet breakup model. The prediction of the most important operating parameters of a venturi scrubber, the pressure drop and the particle collection efficiency was the aim of the studies. Fig. 1 shows the comparison of the overall pressure drop measured by Haller in experiments with our CFD simulations for two gas velocities v_g in the venturi-throat and the liquid load of the flue gas within the typical mass flow range μm = 0.5 .. 2.5.

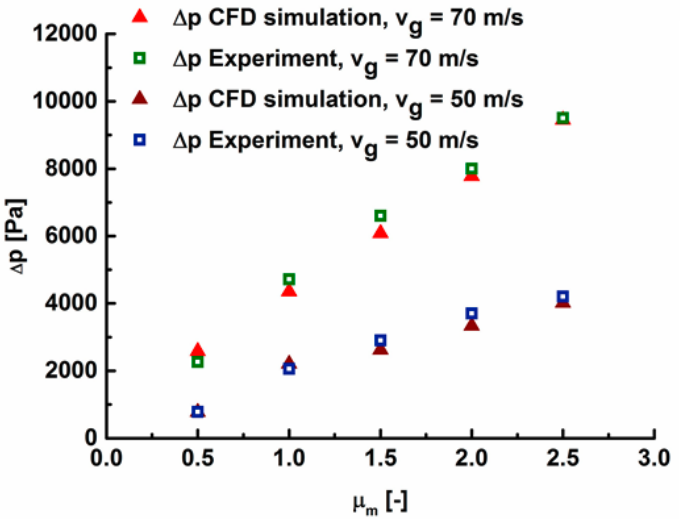

Fig. 1: Comparison of the overall pressure drop measured by Haller in experiments with CFD simulation.

The CFD simulation predicts the overall pressure drop in the venturi scrubber quite well. Further, we investigated the prediction accuracy of the overall and fractional collection efficiency ηg by CFD simulation. Only collision efficiencies of particles with droplets due to inertia were considered.

Fig. 2 shows the comparison of experimental data with CFD simulation results.

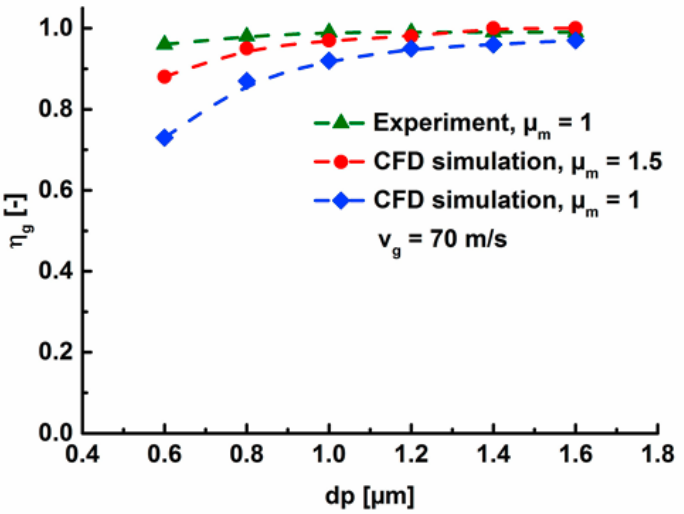

Figure 2: Comparison of the fractional collection efficiency determined by experiments with CFD simulation.

The prediction accuracy of the fractional collection efficiency of particles with diameters greater than 1 μm is very high. However, the CFD simulation results for submicron particles are rather disappointing. The deviation to experimental data can be explained by the transitional complex shape of fluid elements during drop breakup and their additional collection effect due to intermediate large specific surfaces. This process is not yet implemented into the CFD simulation and will be considered in future work.

Contact:
damian.pieloth@bci.tu-dortmund.de
gerhard.schaldach@bci.tudortmund.de
peter.walzel@bci.tu-dortmund.de

Publications:
D. Pieloth, B. Kohnen, G. Schaldach, P. Walzel,
Chemie Ingenieur Technik 2012, 84 (1-2), 127-137

D. Pieloth, T. Neumann, G. Schaldach, P. Walzel,
Chemie Ingenieur Technik 2013, 85 (12), 1888-1895

Residence Time in Hot Melt Extrusion

Monitoring and Modelling of a Pharmaceutical Process

Jens Wesholowski, Elena Reitz, Helmut Podhaisky, David Ely and Markus Thommes

The product quality of pharmaceuticals manufactured by Hot Melt Extrusion with co-rotating twin screw extruders is frequently determined by the residence time and residence time distribution. In order to evaluate these crucial process parameters an experimental setup and a corresponding mathematical model were developed. The residence time was determined by introducing a tracer into the hopper of the extruder, and the measured concentrations at the extruder die were fitted to the residence time model. Several parameters were derived to characterize the extrusion process including the dead time, the apparent mixing volume and a transport related axial mixing.

The continuous extrusion process is modelled as the convolution of mass transport (Fig. 1a) and mixing (Fig. 1b). Both processes occur at all locations within the extruder, from the feeding zone to the die (Fig. 1c). The concentration at the die (Eqn. 1) is determined by the transport process described by an error function, and a mixing process characterized by an exponential decay. Both processes are controlled by four parameters (Eqn. 2-5) and the initial concentration c_0. The process parameters are determined by the dead time t_{dead}, dead volume V_{dead}, mixing volume V_{mix}, flow rate $\dot{V}$ and the width of the residence time distribution σ.

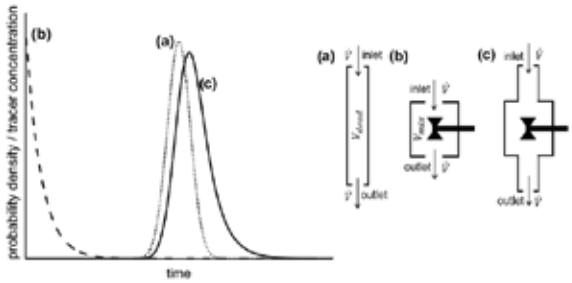

Figure 1: a) Transport process b) Mixing Process c) coupled function.

$$y(t) = c_0 \cdot \frac{1}{2} \cdot e^{k(0.5b_1 - b_2)} \cdot \operatorname{erfc}\left(\frac{b_1 - b_2}{\sigma\sqrt{2}}\right) \quad (1)$$

$$b_1 = k\sigma^2 \quad (2)$$

$$b_2 = t - t_{dead} \quad (3)$$

$$k = \frac{\dot{V}}{V_{mix}} \quad (4)$$

$$t_{dead} = \frac{V_{dead}}{\dot{V}} \quad (5)$$

The extrusion experiments were conducted with a co-rotating twin-screw extruder from Leistritz, Mikro 27GL-28D, for several process conditions.

Xylitol and Copovidone served as model compounds and Theophylline as tracer.

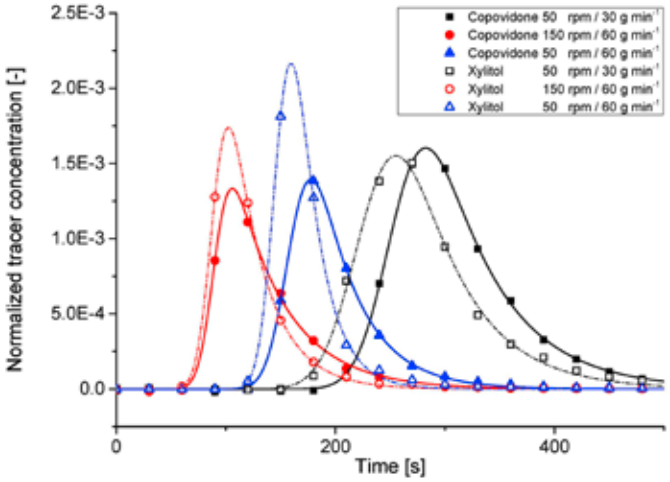

Figure 2: Experimental (symbols) and model data (lines) for the residence time distribution of copovidone (full symbols, straight lines) and xylitol (empty symbols, dotted lines).

Excellent agreement was observed between the measured results and the residence time distribution model (Fig. 2). The developed mathematical model is an excellent description of the extrusion process demonstrated by its high reproducibility in combination with high coefficients of determination and prediction.

Correlations were also observed between the process variables of powder feed rate, screw speed and model compound and the residence time of the extrusion.

In conclusion, the newly developed two compartment model exhibited much better agreement with the experimental data than commonly used residence time distribution models, such as the tanks-in-series or the axial dispersion models.

Publications:
Elena Reitz , Helmut Podhaisky , David Ely , Markus Thommes, European Journal of Pharmaceutics and Biopharmaceutics, 2013, 85, 1200-1205

Contact:
jens.wesholowski@bci.tu-dortmund.de
markus.thommes@bci.tu-dortmund.de

Fluid Separations (FVT)

Chromatographic Separation of Biomolecules

Investigation of Adsorption Behavior of amino acids on polymeric chromatography materials

Marlene Fuhrmeister, Tim Zeiner, Andrzej Górak

Chromatographic purification processes play an important role in the downstream processing of biomolecules. Here the ion exchange chromatography is a reliable platform for the polishing of biomolecules providing mild separation conditions, good selectivity and high capacities. But up to now the adsorption mechanism of biomolecules in chromatographic processes is not fully understood. For this reason high throughput experiments are necessary to gain relevant parameters as pH value or salt content. To reduce the experimental effort the investigation of adsorption behavior of biomolecules in chromatographic processes is necessary. For a better basically understanding and description an adsorption model based on a thermodynamic framework is developed.

Polymeric adsorbents are often applied for adsorption of biomolecules. In dependence on the degree of crosslinking a polymeric network is able to absorb large amounts of water (Figure1). The equilibrium of swollen polymer and the liquid phase can be influenced by the temperature and ionic interactions.

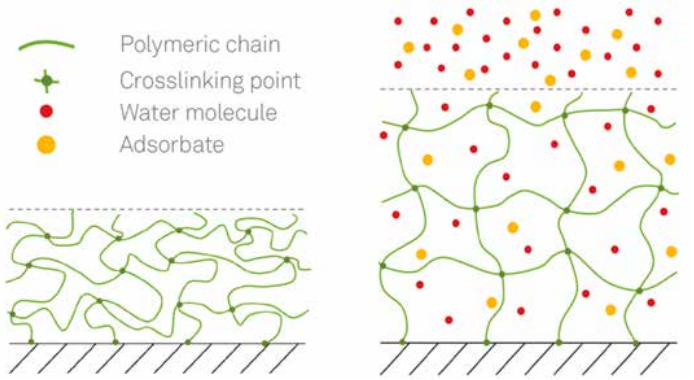

Figure 1: Unswollen polymeric network (left) in comparison to a swollen polymeric network in contact with a solvent and an adsorbate (right).

To consider the swelling behavior and other properties of the components and the multi component system a model based on a thermodynamic approach is developed. With this approach the influence of the component properties on the adsorption behavior and the process parameters as temperature, pH value and ionic strength can be modeled. As a basis a gE-model based on the Flory-Huggins approach is used for which a limited number of model parameters have to be fitted to experimental data.

The model is able to describe the ternary adsorption system as well as the binary subsystems, for example solid liquid equilibria, liquid liquid equilibria or the swelling behavior of the polymeric adsorbent. Most model parameters can be fitted to experimental data of the phase behavior of the binary subsystems. Experimental and modeled data of the adsorption behavior of phenylalanine on XUS-40323 adsorbent is shown in Figure 2b.

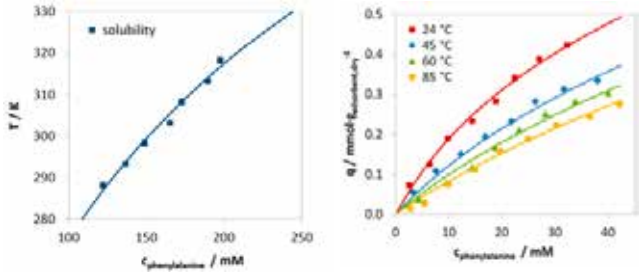

Figure 2: a) Experimental data and modeled solubility of phenylalanine in water; b) Experimental data and modeled adsorption isotherms of phenylalanine on XUS-40323 adsorbent in water.

The model is able to describe the solubility of phenyl-alanine in water (Figure 2a) as well as the temperature dependency of the adsorption. Also it is possible to describe the swelling behavior of the polymeric adsorbent. For model parameter fitting only a few experimental data points of the adsorption behavior are necessary.

The structure of this model allows the model parameter estimation by independent experimental data of phase equilibria of the underlying binary systems, swelling equilibria of the polymeric adsorbent and adsorption experiments. On the basis of the model an approach for an experimental design with defined and limited number of experiments can be developed to fit the model parameters and to reduce the experimental effort. Afterwards it is possible to model interesting operating points and do sensitivity analyses.

On the basis of the adsorption model a chromatography model can be developed by combination with an appropriate mass transfer model. Other possible applications are the adsorbent selection for a given separation task with a minimal number of experiments or to define suitable adsorbent properties by modeling.

Contact:
marlene.fuhrmeister@bci.tu-dortmund.de
tim.zeiner@bci.tu-dortmund.de
andrzej.gorak@bci.tu-dortmund.de

Intensified separation processes

Systematic characterisation of rotating packed beds

Kolja Neumann, Philip Lutze, Andrzej Górak

The intensification of processes and unit operations in the chemical industry offers new ways to face the challenges coming along with the need for more efficient, compact and flexible production processes. One promising technology which combines a compact design with flexibility are rotating packed beds (RPBs), operating at high gravitational forces. By generating a centrifugal field an intense contact between a liquid and a gas is provided, leading to very good mass transfer rates and high capacities. The scope of the proposed project is to evaluate and quantify the potential of the RPB technology to improve separation processes. The objective is to develop the fundamental know-how and understanding of RPBs and to demonstrate its applicability for selected industrial cases.

Well established conventional separation technologies are packed bed absorption towers for gas-liquid separation or packed bed distillation columns for vapor-liquid separation. These technologies operate in the gravita-tional field whereas the operating windows are limited due to flooding. Applying a centrifugal field by rotation in RPBs, results in a significant increase of the gravitational force enlarging the operational window. In counter current operation gas flows through the donut-shaped rotating packing from the outside to the middle of the rotor. Simultaneously liquid is sprayed into the eye of the rotor and flows driven by the centrifugal movement to the outside of the rotor (see figure 1).

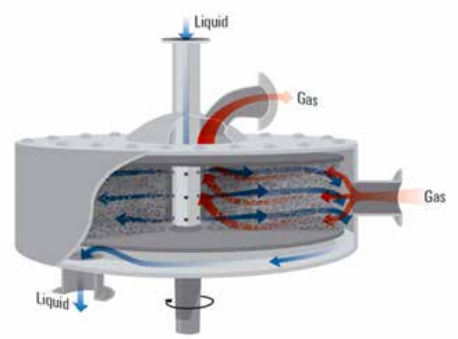

Figure 1: Gas-liquid contacting in counter-current operation in a rotating packed bed (RPB)

The advantages are high gas loads and turbulences producing small droplets or gas bubbles leading to high interfacial areas without early flooding. Thus the mass and energy transfer within and between the phases is intensified. Direct benefits are the increased performance, the enlargement of the operating window, the flexibility of the rotational speed and therefore of the separation efficiency, and the high capacity at a very compact design. In order to evaluate the potential of RPB technology a detailed RPB model was first developed and successfully validated [1] at the chair of fluid separations. Further-more, Sudhoff et al. [2] published a comprehensive study incorporating the developed RPB model and an extensive analysis of the design and flexibility of rotating packed beds for distillation. Just a few fundamental studies of the hydrodynamics and mass transfer in RPBs, have been reported but a general systematic characterisation has not been made and is now focus of the research. In order to characterise the RPB technology the hydrodynamics, operational window and mass transfer are investigated systematically. Additionally findings in literature (see figure 2a) are compared with own experimental results (see figure 2b) often showing different results.

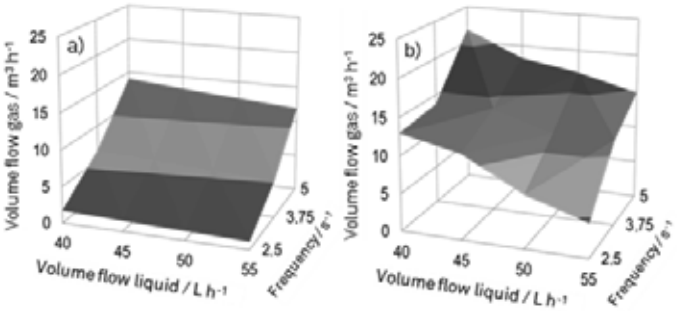

Figure 2: Operating window for a rotor height of 10 mm with increasedviscosity of 560 mPas, a) according to wallis equation [3] b) experimentally determined flooding points in pilot plant

Especially the influence of operational and design parameters on the hydrodynamics and on the mass transfer is investigated to improve the RPB design. Currently performed experiments showed a good performance of RPBs for CO2 absorption in viscous media. Later on new rotor geometries and models for different unit operations will be developed to enhance the understanding of the RPB technology.

Contact:
kolja.neumann@bci.tu-dortmund.de
andrzej.gorak@bci.tu-dortmund.de

Publications:
[1] D. Sudhoff, K. Neumann, P. Lutze
Computer Aided Chemical Engineering, 2014, 33, 1303–1308

[2] D. Sudhoff, M. Leimbrink, M. Schleinitz, A. Górak, P. Lutze,
Chemical Engineering Research and Design, 2015, 94, 72-89

[3] S. Rajan, M. Kummar, M. Amsari, D. Rao, N. Kaistha
Industrial Engineering Chemical Research, 2010, 50, 986-997

Membrane Contactors

A flexible tool of process intensification

Mathias Leimbrink, Mirko Skiborowski, Andrzej Górak

Membrane Contactors (MC) are a promising tool for the intensification of fluid separation processes and provide the potential to meet current requirements on sustainability in the chemical industry. MC provide a defined and large interfacial area (IA), which is orders of magnitude higher than for conventional equipment and independent of the flow conditions. This independency allows for a flexible operation in MC equipment that can help to compensate for fluctuations during operation. Until now, MC are only used in niche applications as a general design method is still unavailable, providing the motivation for the current work.

To determine the potential of MC as a representative of intensified and flexible separation equipment, three major challenges have to be tackled. First, a deeper knowledge of the occurring mass transfer phenomena has to be gained by systematic experimental investigations. Second, feasible fields of application need to be identified in order to demonstrate the potential of MC to intensify processes in comparison to conventional equipment. Third and finally, a model has to be developed which is capable of representing the specific mass transfer characteristics for a selected application to consider MC during a conceptual process design. These three steps span the scope of the current work (see Fig. 1).

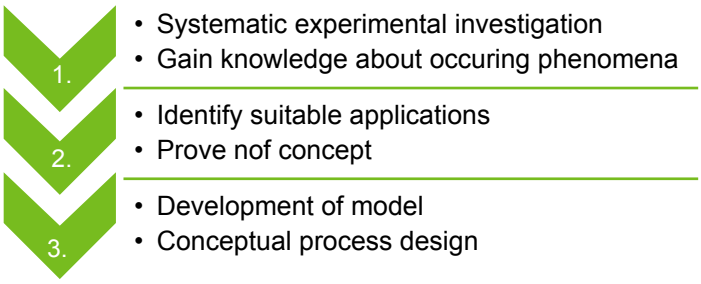

Figure 1: Scope of this work

While MC can be applied as contacting equipment in most fluid separations, leading to improved process efficiencies, they also introduce additional operational constraints. Hereby, the comparably low temperature stability and the need for controlling the transmembrane pressure difference in order to avoid breakthrough of either the liquid or gas phase have to be considered. Especially the latter constraint was identified as crucial limitation concerning the mass transfer performance. Therefore, our work focuses on a systematic characterization of this phenomenon to enable a correct interpretation of mass transfer measurements.

Besides, gaining deeper insights in mass transfer in MC, the identification of potential fields of application is an essential part of this work. Current investigations focus on the enzyme-accelerated reactive absorption of CO2 from flue gas, while alternative applications will be investigated in the future. A scheme of the current process is illustrated in Figure 2.

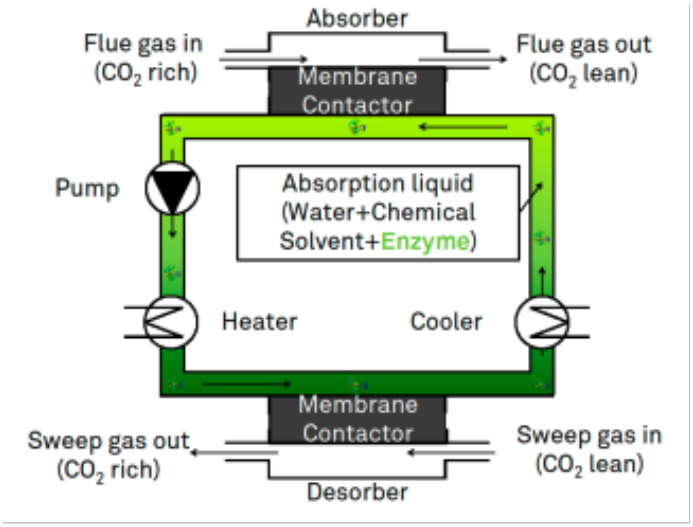

Figure 2: Process scheme of MC and enzyme facilitated CO2 separation

In this process the solvent recovery is the bottleneck due to its high energy consumptions. The application of solvents requiring less energy for recovery is intensively studied but still restricted by low absorption rates. The combination of MC with the enzyme Carbonic Anhydrase can compensate for this low absorption rate and result in an intensified mass transfer. As a result, a significant improvement of energy efficiency can be achieved.

Further case studies, will be identified and evaluated in the future to demonstrate the potential of MC to intensify separation processes. Finally, the compiled information will be transferred to a rigorous modeling of MC-based separation processes. This is necessary to evaluate the performance of MC in comparison to conventional or competing equipment.

Contact:
mathias.leimbrink@bci.tu-dortmund.de
mirko.skiborowski@bci.tu-dortmund.de
andrzej.gorak@bci.tu-dortmund.de

Fluid Mechanics (SM)

Multiphase reactions systems

Mass transfer at free liquid/liquid interfaces

Christian Heckmann, Peter Lakshmanan, Peter Ehrhard

Mass transfer in multiphase systems finds extensive applications in chemical–engineering problems, like chemical reactions, extraction, or adsorption. Liquid-liquid systems take a special position, because the overall mass transfer process is influenced by the mass transfer resistance in both phases – this is a conjugated problem. Furthermore the mass transfer process itself is highly depending on the properties in the mass transfer boundary layer. We developed a new concept that can handle the hydrodynamics and the mass transfer of conjugated mass transfer systems, considering a high resolution at the free interface.

We focus on a two-phase system, consisting of two incompressible immiscible and Newtonian liquids, which are acting as solvents for a solute, which is extracted from one phase to the other. Starting point for the hydrodynamics of the examined two–phase system is an imported steady–state interface. On both sides of this interface separate static computational domains are arranged. Both domains are coupled at the free surface to cpmpute the flow of the considered multiphase system. Coupling conditions arise from the kinematic and dynamic constraints at the free surface. The mass transfer is examined based on the steady-state hydrodynamics of the two-phase system. Dilute concentrations are assumed, so the back-coupling of the mass transfer to the hydrodynamics of the multiphase system can be neglected. Hence transport equations for a passive (scalar) concentration are solved at both sides of the interface. At the liquid/liquid interface, transitions conditions arise from both, the interfacial dissolution equilibrium (according to Herny´s law) and the mass-flux continuity across the interface.

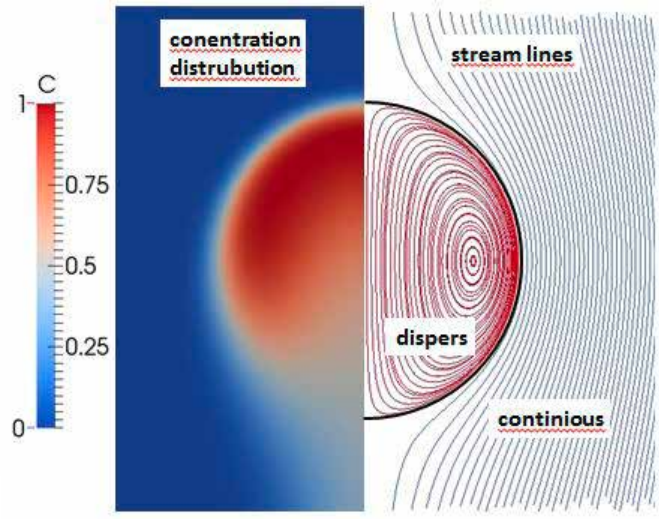

Figure 1: a) Concentration Field for Fo=0.02, D=1 , Re=0.1, initial concentration C_0=1, b) stream lines for Re=0.1.

The dimensionless groups of this problem are the Reynolds number *Re*, the viscosity ratio η, the density ratio λ, the Péclet number *Pe*, the ratio of the diffusion coefficients D and the Fourier number *Fo*. The development and the validation of the numerical simulation model has been done using the extraction process of a free rising spherical droplet in a creeping flow (cf. Figure 1). The transient mass transfer is validated using the theoretical limiting case of the inner problem, corresponding to a negligible mass transfer resistance in the continuous phase ($D \rightarrow \infty$). The simulation results are within the limiting analytical solutions for a stagnant drop and for strong convection ($Pe \rightarrow \infty$), see Figure 2.

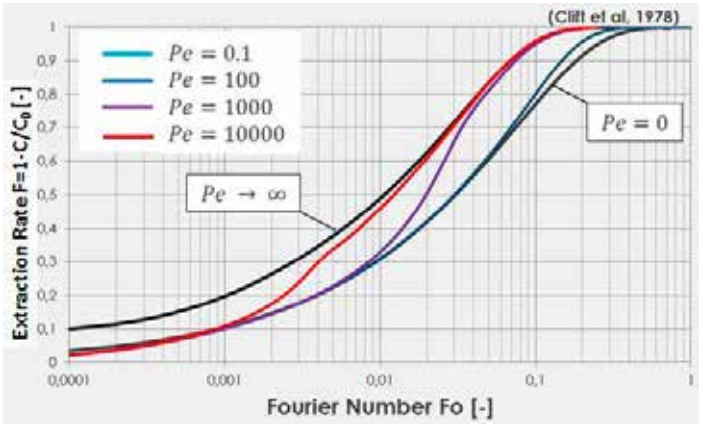

Figure 2: Extraction rate F over dimensionless Time Fo.

The numerical results are overall in good agreement with the corresponding references. The established concept can be applied to any kind of multiphase mass transfer system, which is in agreement with the fundamental assumptions.

Publications:
C. Heckmann, P. Lakshmanan, P. Ehrhard, mass transfer at free liquid/liquid interfaces, PAMM, submitted 2015

Contact:
christian.heckmann@bci.tu-dortmund.de
peter.lakshmanan@bci.tu-dortmund.de
peter.ehrhard@bci.tu-dortmund.de

Jungebad®

Study of dispersion production and droplet-size-distribution

Ann-Kathrin Höffmann, Peter Lakshmanan

WERNER JUNGE developed the Jungebad® apparatus in 1937 based on thoughts from a lecture of Dr. RUDOLPH STEINER from 1920. To obtain a successful therapy, it is useful to generate a large surface-to-volume ratio of the oil. Therefore, small droplets have to be produced which uniformly distribute in the bath and on the skin. The produced oil-dispersion bath activates the self-healing forces and helps to strengthen the ego of patients. To determine the droplet-formation mechanism and the optimal operating point of the apparatus, a high-speed camera is used. Furthermore, the droplet-size-distribution is analyzed.

The oil dispersion is formed within the Jungebad® apparatus by a capillary which disperses oil in a rotating water flow. Figure 1 shows the apparatus and water flow direction.

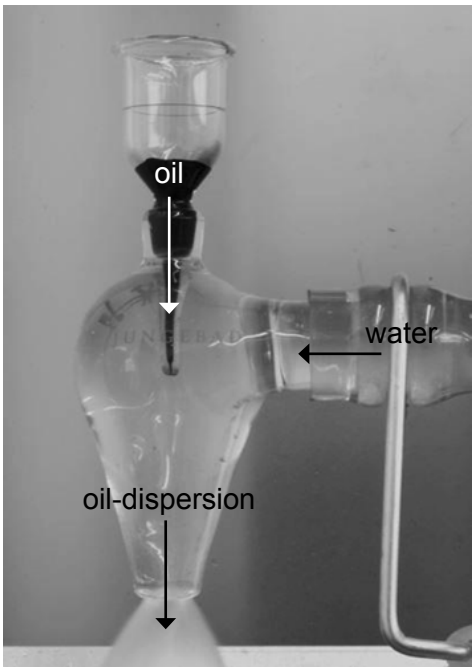

Figure 1: Jungebad® apparatus.

For different water volumetric flow rates, the mechanism of droplet formation at the capillary changes. Figure 2 demonstrates two different droplet formation mechanisms for volumetric flow rates of 5 l/min and 15 l/min.

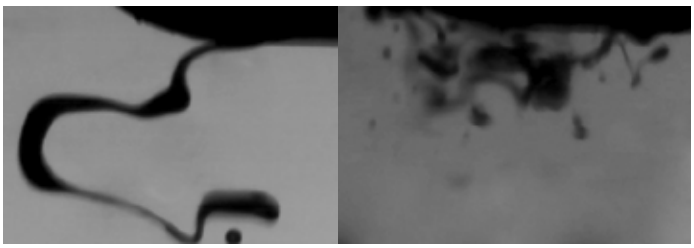

Figure 2: Droplet formation at the capillary for inlet flow rates of 5 l/min (left) and 15 l/min (right), captured by a high-speed camera.

At low volumetric flow rates, the oil builds one oil thread at the capillary which then breaks up into droplets. At high volumetric flow rates, the oil threads split into several smaller threads which then break up into droplets immediately after the capillary.

To analyze the droplet-size distribution the water-oil-dispersion flows between two glass panes, where the droplets can be observed, measured, and counted. Figure 3 presents the resulting droplet-size distribution for several volumetric flow rates. It is evident that the droplet-size distribution is essentially not changing with increasing volumetric flow rates.

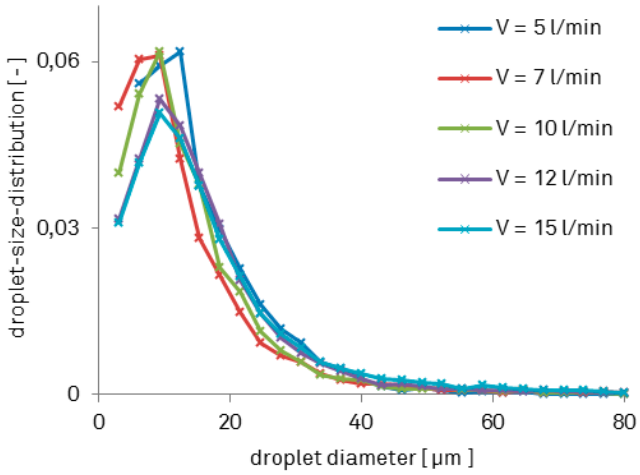

Figure 3: Droplet-size distribution of oil droplets formed by the Jungebad® apparatus.

In summary, the droplet formation mechanism at the capillary changes with the inlet volumtric flow rate but the droplet-size distribution is hardly affected. Mistakes in the application by the user are not possible and the optimal operating point is reached at high inlet volumetric flow rates to quickly fill the bathtub.

Contact:
ann-kathrin.hoeffmann@bci.tu-dortmund.de
peter.lakshmanan@bci.tu-dortmund.de

Stability analysis of a non-isothermally spreading droplet on a rotating disk

A simple and novel way to suppress the finger instability in spin-coating

Konrad Boettcher, Timo Externbrink, Peter Ehrhard

Spin-coating is widely used in coating industries, mostly in the production of semiconductors by coating wafers. In this process a liquid droplet is placed on a solid which has to be coated (mostly a perfectly-plane wafer). The solid starts to rotate and centrifugal forces spread the liquid. After that the liquid gets dried and the process is completed. During the spreading there is a fluid-mechanical instability that may occur: The droplet forms an annular ring (the so-called capillary ridge), which breaks up into several sub-ridges. After that liquid fingers develop from the sub-ridges and the rest of the liquid flows through these fingers, leaving the area between the fingers unwetted and due to this the coating process fails. Investigating the influence of temperature gradients, we found a simple way to suppress this finger instability.

The problem consists of a droplet on a solid plane surface, surrounded by a gas. A free interface is involved between the liquid and the gas. For modeling, we use the continuity, the Navier-Stokes, and the heat transport equation to describe the physics. As these droplets are extremely thin, surface effects are more important than volume effects, whereas surface tension depends on temperature and decreases linearly. The spreading is treated dynamically and a macroscopic law (the generalized Tanners law) is used to link the speed of the wetting front to the apparent dynamic contact angle. Due to the geometric disparity, the difficulty of interface reconstruction (which is crucial for the wetting law), and a stress singularity at the moving contact line, standard CFD methods fail in computing such problems. The lubrication approximation and slippage is engaged to circumvent these problems.

In the base state, no perturbations are present and the droplet spreads rotationally-symmetric due to centrifugal, gravitation, and wetting forces. The centrifugal forces form a capillary liquid ridge near the wetting front. Temperature gradients lead to gradients in surface tension, which produce a shear stress, the so-called Marangoni-stress. The free interface, computed with the theoretical model, matches experimental results gained by using a chromatic confocal measurement system quite well.

To investigate the finger instability, perturbation theory is engaged to check the linear stability of the base state. It is shown, that several modes (cf. fig. 1) get successively unstable.

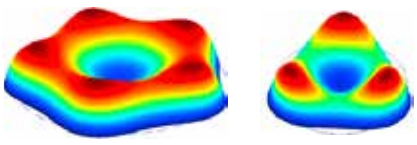

Figure 1: Droplets with growing modes 5 and 3.

This corresponds to the experimental observation, where one finger forms after the other. While centrifugal forces are increasing the growth rate of the instability, gravity and surface tension have a surface leveling, and therefore damping influence. Central cooling of the disk amplifies lower modes and damps higher modes. The effect gets more pronounced for higher gradients and is a result of two counter-acting effects: i. Marangoni-stresses pull the liquid back from the front, ii. Leveling effects of surface tension decrease with higher spreading radii as the disk gets warmer. Obviously, the second effect is more important for higher modes, as the interface is more corrugated. Uniform cooling of the plate (or heating the gas) leads to Marangoni-stresses from the top of each sub-ridge and levels the corrugation. As there is no amplifying effect, all modes get damped. Therefore, cooling the disk or heating the gas seems to be a simple way to suppress the finger instability in spin-coating.

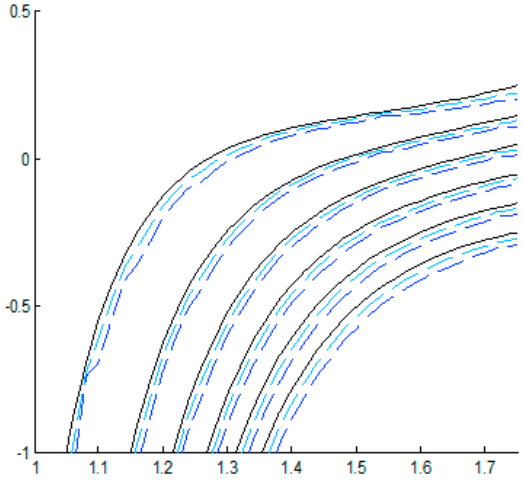

Figure 2: Scaled growth rate of the modes 2 - 7 against scaled mean spreading radius. Solid black lines reflect the isothermal case. The blue dashed lines reflect a cooled disk (dark blue: stronger influence)

Publications:
K. Boettcher, P. Ehrhard, European Journal of Mechanics – B/Fluids 2014, 43, 33 - 44

K. Boettcher, T. Externbrink, Proceedings in Applied Mathematics and Mechanics 2015, submitted

Contact:
konrad.boettcher@bci.tu-dortmund.de
peter.ehrhard@bci.tu-dortmund.de

Wetting phenomena in porous layers

Numerical investigation of a liquid displacing a gas in multiple thin porous layers

Tim Neumann, Konrad Boettcher, Lutz Gödeke, Peter Ehrhard

The cells of a lithium-ion battery may be described as thin porous layers on the electrodes made of copper and aluminum, with a thin and permeable layer separating these two porous domains, so that one elementary cell is composed of three porous layers with heterogeneous characteristics. The whole battery consists of about 100 of these elementary three-layer cells. For optimizing the filling-process of such batteries with the electrolyte, a numerical model of one elementary cell is established.

All relevant physical forces are implemented, based on models for porous packages of spheres in a square bounded geometry. The viscous forces are taken into account using the generalized Darcy´s law by adding $\vec{S}_{viscous}=-\frac{\mu}{k}\cdot\vec{w}$ in the Navier-Stokes equations as a momentum sink, with the permeability k, proportional to the square of the hydraulic diameter for a package of spheres, the dynamic viscosity μ and the mean velocity vector $\vec{w}$ of the liquid flowing in the pores of a porous media. For the filling-process Reynolds numbers $Re_k<0.001$ are expected (Re_k build with the characteristic length $\sqrt{k}/\varepsilon^3$, with the porosity ε). In this range the inertial forces can be neglected. With respect to the two-phase flow, the Volume-of-Fluid method is used to localize the interface of the wetting liquid. The wetting force is implemented by using a capillary model considering the shape of cavities in the porous media, leading to the momentum source $\vec{S}_{wetting}=-\sigma\cdot F\cdot\nabla\Phi$ which is added to the full porous form of the Navier-Stokes equations. Here, F is a wetting coefficient, dependent on the porous matrix, σ is the surface tension and ∇Φ is the gradient of the volume fraction of the wetting phase.

For the thin layers of the electrodes, the wall effect is considered. The porosity is getting high near the boundaries. Modell experiments with similar particle size distributions as in the layers are conducted to get the porosity as a function of the wall distance from the solid electrodes; the porous separator is modeled with a constant porosity. In the numerical model, on the one hand, the mobility of the contact line on the solid electrodes is assured. On the other hand, the no-slip condition for the wetting phase is fulfilled.

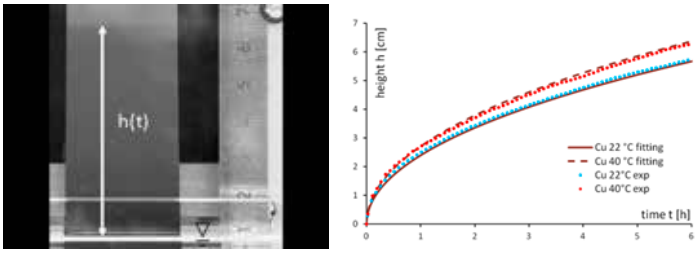

Figure 1: Capillary rise in thin porous layers on the copper electrodes for two different temperatures. The experimental results for the height of the wetting front by time are fitted to determine *k* and *F*.

For correction of the physical parameters, the permeability k and the wetting coefficient F, which are calculated with an ideal sphere package model, capillary rise experiments are conducted with the three different porous layers. The electrodes and the separator are positioned parallel to the gravity vector, ending in a glass reservoir filled with silicone oil. The experiments are done in a saturated atmosphere. The height of the liquid front is measured in time for different temperatures. The mathematical description on the capillary displacement flow of the wetting phase in the porous media for low Reynolds numbers is solved analytical, leading to an equation describing the height of the wetting front in time.

$$h(t)=\frac{\sigma F}{\rho g}+e^{-\left[1+\sigma F\cdot\ln(-\sigma F)+\frac{k(\rho g)^2}{\mu\ \sigma F}t+\mathrm{LambertW}\left(e^{-\left[1+\frac{k(\rho g)^2}{\mu\ \sigma F}t\right]}\right)\right]}$$

The experimental results are fitted to this equation, as seen in figure 1, to determine the parameters k and F.

The implementation is validated; the solution of the capillary rise in one of the layers is compared with the results of the numerical investigation with deviations smaller 1 % in figure 2.

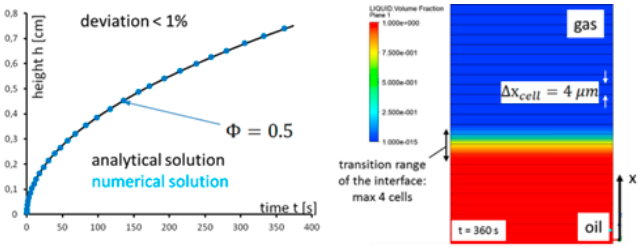

Figure 2: Capillary rise in the separator layer. Comparison of the height of the wetting front as function of time, taken from the analytical solution and taken from the numerical simulation.

Contact:
Tim.Neumann@bci.tu-dortmund.de

Publications:
T. Neumann, K. Boettcher, Proceedings in Applied Mathematics and Mechanics 2015, submitted

Technical Biochemistry (TB)

Endophytic community biosynthesis

Plant compound maytansine has a microbial biosynthetic origin

Parijat Kusari and Oliver Kayser

Given the central role of chemical crosstalk in plants and endophytes, it is compelling that certain compounds or their precursors formerly believed to be synthesized only by plants or exclusively considered plant metabolites can be produced by endophytes or other plant-associated microorganisms. The basic objective of our work was to verify whether the important anticancer and cytotoxic compound maytansine is produced entirely by Putterlickia plants or by their endophytic microflora.

Endophytes are a diverse group of microorganisms that colonize the internal tissues of plants without any manifestation of disease and engage in mutualistic association with the host plants. The main objective of our work was to experimentally prove whether maytansine is produced by *Putterlickia verrucosa* and *Putterlickia retrospinosa* plants, or by the endophytic microbial community harbored in them. We evaluated the fermentation products of endophytic community harbored in different tissues of *Putterlickia* plants by a combination of high performance liquid chromatography high-resolution mass spectrometry (HPLC-HRMSn), matrix assisted laser desorption ionization imaging high-resolution mass spectrometry (MALDI-imaging-HRMS) and gene discovery methods to characterize the production of maytansine.

After isolating the endophytic community from different tissues of *Putterlickia* plants, we used the combination of HPLC-HRMS^n and MALDI-imaging-HRMS, a maytansine-specific selective microbiological assay, and gene discovery methods to elucidate the source and site of maytansine biosynthesis. Initially, HPLC-HRMS^n analysis revealed the production of maytansine by root endophytic community. This was further coupled to a microbiological assay (bioautography) using maytansine-sensitive type strain *Hamigera avellanea*. Finally, the presence of AHBA synthase gene in the root endophytic communities of *Putterlickia* plants coupled to its absence in host plants confirmed that maytansine is a biosynthetic product of root endophytic community. Additionally, MALDI-imaging-HRMS demonstrated the accumulation of maytansine produced by endophytes in the root cortex of both the host plants.

Thus far, our study reveals maytansine is actually a biosynthetic product of root-associated endophytic microorganisms and opens up further questions about the broad ecological role of maytansine in nature and the endophytes residing in distinct ecological niches.

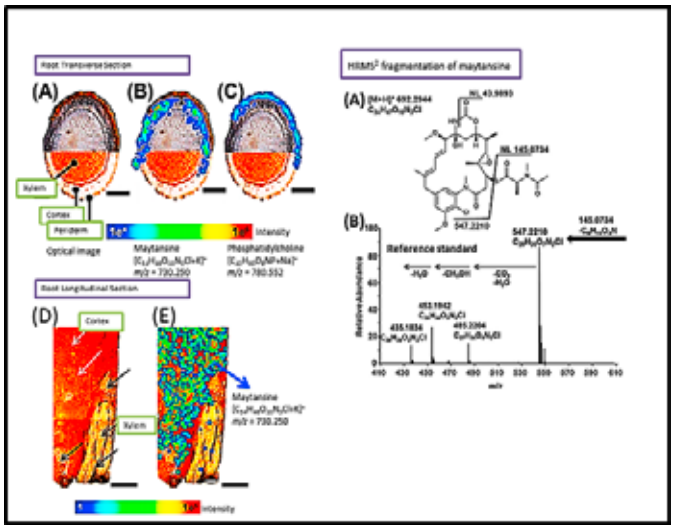

Figure 1: Maytansine produced by the endophytes is typically accumulated mainly in the root cortex of both plants, but not in other tissues

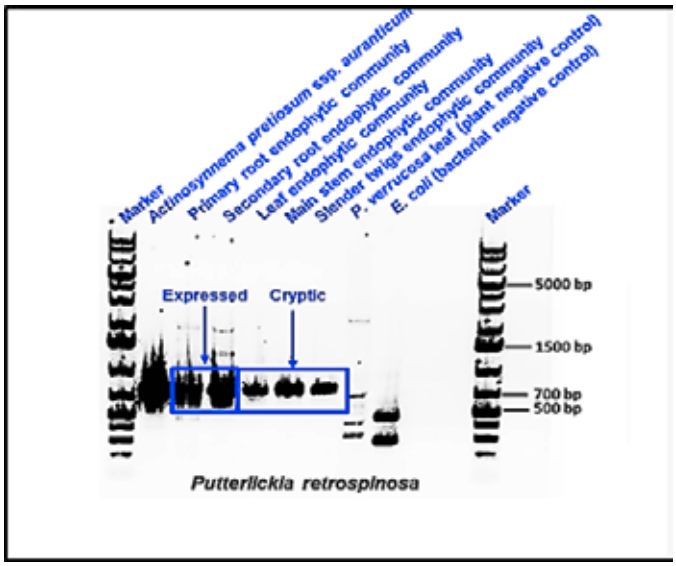

Figure 2: Confirmation of maytansine production by root bacterial endophytic community by gene discovery

Contact:
Parijat.kusari@bci.tu-dortmund.de
Oliver.kayser@bci.tu-dortmund.de

Collaborators:
Souvik Kusari (s.kusari@infu.tu-dortmund.de)
Michael Spiteller (m.spiteller@infu.tu-dortmund.de)
Institute of Environmental Research (INFU), Department of Chemistry and Chemical Biology of TU Dortmund

Publications:
[1] Kusari S., Lamshöft M., Kusari P., Gottfried S., Zühlke S., Louven K., Leistner E., Hentschel U., Kayser O., Spiteller M. (2014) Endophytes are hidden producers of maytansine in Putterlickia roots. J Nat Prod 77:2577-2584

Biocontrol efficacies of endophytes

Similar and discrete traits of endophytes harbored in plants with similar secondary metabolite production

Parijat Kusari and Oliver Kayser

It is immensely important to understand the reaction and stability of endophytes in any microbe-microbe interactions due to biotic selection pressures, outside the host environment. It is compelling that similar biosynthetic principles apply phylogenetically unrelated plants (like Radula marginata and Cannabis sativa L.) with regard to production of structurally similar compounds. The basic objective was to evaluate the probable contributions and capabilities of endophytes harboured in liverwort Radula marginata in aiding host fitness against the pathogens.

Liverworts are small, simple and non-vascular plants existing in almost all ecosystems, though they are abundant in the tropical niches. However, these small plants are highly rich in terpenoids and aromatic compounds. Recent investigations on *Radula marginata* led to the identification of bibenzyl cannabinoids (namely perrottetinene and perrottetinenic acid), with structural similarity to tetrahydrocannabinol, the major psychoactive secondary metabolite of *Cannabis sativa* L. plants. Taking cues from our previous work on the endophytic community of *C. sativa*, this study compares and evaluates the ecological significance and antagonistic potential of bacterial endophytic community of *R. marginata* as compared to that of *C. sativa*.

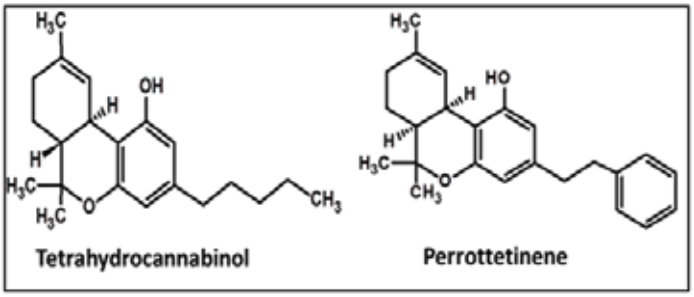

Figure 1: Structurally similar secondary metabolite in *Cannabis sativa* L. and *Radula marginata*

The endophytes were challenged against *B. cinerea* and *T. roseum*, under five different media conditions to justify and compare the potent benefits and challenges encountered by endophytic isolates against the pathogens. Some isolates demonstrated physical defense strategies by causing malformation of pathogen mycelia on contact. Others were able to perceive unfavorable conditions long before physical proximity, and displayed chemical defense by either releasing visible exudates, forming inhibition zone (halo) or even producing secondary metabolites in form of dark brown to black bands. Although *Bacillus* sp. is quite commonly found in various ecological niches, exhibiting an endophytic lifestyle in two different host plants with similar biosynthetic principles is noteworthy. To gain a deeper insight into the significance of presence of similar bacterial species, the bacterial endophytic isolates were further exploited for their efficacies in retaining certain 'defensive' functional traits like biofilm formation.

Endophyte Strain number	Antagonistic inhibition (% inhibition) against *Botrytis cinerea* in five different media					Different endophyte-pathogen interactions under five different media				
	WA	SA	PDA	MEA	NA	WA	SA	PDA	MEA	NA
R1	0	15	22	-10	55	4	2	2	1	3
R2	20	-29	33	10	NG	4	1	3	1	12
R3	20	0	11	20	82	4	3	1	1	4

Code	Endophyte-pathogen interaction descriptions
A	Both endophyte and pathogen grow towards each other, but growth stopped and mycelia of pathogen malformed as their mycelia came in physical contact; no sporulation; no color alteration of mycelia; no release of visible exudates; no inhibition zone (no halo)
B	Both endophyte and pathogen grow towards each other, but growth stopped and mycelia of endophyte malformed as their mycelia came in physical contact; no sporulation; no color alteration of mycelia; no release of visible exudates; no inhibition zone (no halo)

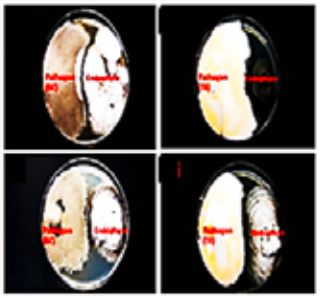

Figure 2: Antagonistic potential (inhibition calculations) of endophytic isolates harbored in *Radula* against phytopathogens

Thus far, our work underlines the similar and discrete traits of endophytic community of plants from different geographical niches with similar secondary metabolite (cannabinoid) production.

Contact:
Parijat.kusari@bci.tu-dortmund.de
Oliver.kayser@bci.tu-dortmund.de

Collaborators:
Souvik Kusari (s.kusari@infu.tu-dortmund.de)
Michael Spiteller (m.spiteller@infu.tu-dortmund.de)
Institute of Environmental Research (INFU), Department of Chemistry and Chemical Biology of TU Dortmund

Publications:
[1] Kusari P., Kusari S., Spiteller M., Kayser O. (2014) Biocontrol potential of endophytes harbored in Radula marginata (liverwort) from the New Zealand ecosystem. Antonie van Leeuwenhoek 106: 771-788

Technical Chemistry (TC)

Reactive extraction of terpenyl amines using formic acid

An efficient process alternative for the purification of amines from renewable resources

Tobias Färber, Arno Behr

The reactive extraction of terpenyl amines was investigated in batch and continuous scale using a reversible acid-base-reaction. This process alternative allows the efficient and gentle separation of the terpenyl amines from the solvents and reactants in the reaction mixture. The reactive extraction was verified on a continuous scale during miniplant operation.

Terpenyl amines (TPA) are long-chain aliphatic amines that can be generated from renewable resources. The hydroamination of the renewable β myrcene with morpholine as model substrates generates terpenyl amines in high yields. One of the main challenges of the production lies within the purification of the terpenyl amines from the product mixture. After the reaction the products reside in the non-polar solvent phase along with the substrate β-myrcene, which has not reacted. The purification by distillation is not feasible, as the boiling point of the terpenyl amines is relatively high (>250°C). The reactive extraction is an efficient process alternative that allows the separation without the application of high temperatures or extremely low pressures.

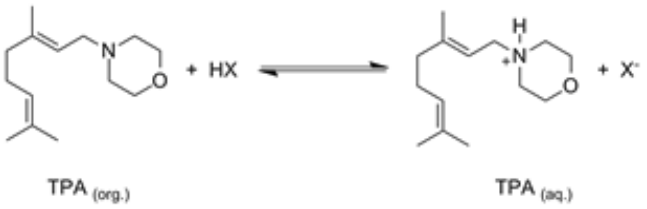

Figure 1. Acid-base-reaction (simplified)

The reaction of the TPA with an acid (Figure 1) protonates the amines, makes them water soluble and extracts them from the non-polar solvent phase into a second water phase. This acid-base-reaction is reversible, if the correct acid is chosen. This way the reaction can later be reversed by the removal of the acid. The application of elevated temperatures (T = 100 °C) and a reduced pressure (p = 10 mbar) removes the acid, yielding the terpenyl amines in high purity (>98%).

A primary acid screening showed that a compromise between extraction efficiency ($n_{amine,extracted}$:$n_{amine,total}$) and the amine recovery has to be made. Strong acids lead to a nearly complete extraction, but amine recovery is very difficult. As a result carboxylic acids were selected as they showed moderate extraction efficiencies (Y_{Ex}= 63%) and good amine recovery.

This concept was then validated in semi-batch operation using an acrylic glass mixer-settler prototype to look into the unknown phase separation properties (separation time, phase behavior, foaming, etc.). This concept was then refined and a modular steel mixer-settler constructed, that allowed the operation under elevated pressure in the miniplant (Figure 2).

Figure 2. 3D-rendering of finished steel mixer-settler for operation under elevated pressure

Using these prototypes the extraction efficiency and the minimal necessary formic acid:TPA ratio was determined (Figure 3). Very high extraction efficiencies (Y_{Ex}>95%) can be achieved at acid:amine ratios above 2:1. Lower acid concentrations lead to the decline of the extraction efficiency.

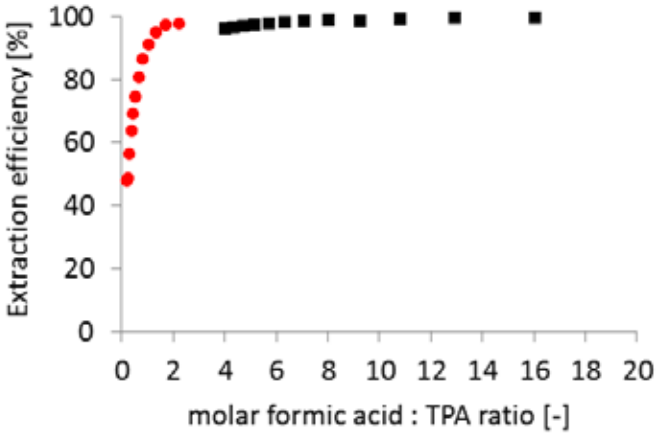

Figure 3. Semi-batch reactive extraction

Finally the steel mixer-settler was validated during miniplant operation in the continuous hydro-amination of β-myrcene, where it successfully extracted the desired terpenyl amines.

Contact:
arno.behr@bci.tu-dortmund.de

The first Tandem Hydroformylation/Acyloin Reaction

Yielding Acyloins directly from Olefins

Karoline A. Ostrowski, Thiemo A. Faßbach, Arno Behr and Andreas J. Vorholt

A novel, atom efficient, tandem catalysis was developed yielding acyloin products (α-hydroxy ketones) directly from olefins under hydroformylation conditions. The combination of a metal catalysed hydroformylation and an organocatalysed acyloin reaction provides three atom efficient C C bond formations to linear, multifunctional molecules via linkage of the intermediate n-aldehydes.

The application of two or more different catalysed reactions in one reaction vessel is called tandem catalysis, which is still a quite new and little explored field in chemistry. Tandem catalyses save effort, time, energy and resources by not isolating or purifying intermediates. Due to these advantages, tandem catalysis has become a flagship for sustainability.

Herein, we present the first tandem hydroformylation/acyloin reaction, which forms acyloins directly from terminal alkenes and syngas within one preparative step (Figure 1).

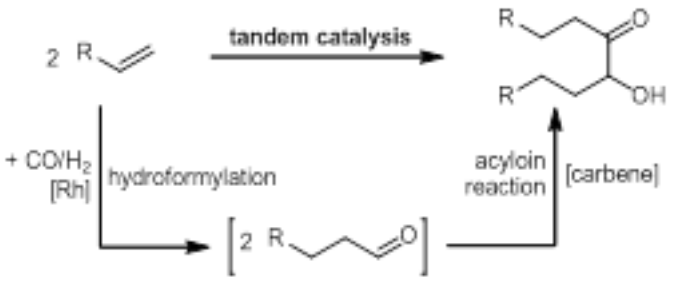

Figure 1. Acyloin reaction under hydroformylation conditions in tandem catalysis.

Key to success in this new tandem catalysis is the combination of a rhodium catalysed hydroformylation yielding aldehydes with high *n/bra* (*bra* = *branched*) ratio and the selective carbene catalysed transformation of these intermediates to acyloin products. $Rh(CO)_2acac$ is used as precursor together with a phosphine ligand. The applied organocatalyst is derived readily from the coenzyme thiamine/vitamin B_1 by in situ deprotonation with base, e.g. triethylamine. Thiamine was chosen due to having no GHS hazard statements and its wide availability, e.g. in yeast.

After an optimization of the reaction conditions, the scope of the developed tandem catalysis was explored by applying different 1-alkenes. To prove synthetic usefulness, besides aliphatic 1 alkenes, also different functionalised 1-alkenes were converted (X_{Olefin}) to their corresponding acyloins (Y_{Acyl}). A selection of applied olefins is given in Table 1.

olefin	product	X_{Olefin}	Y_{Acyl}
		100	73
		98	76
MeO	MeOOC MeOOC	100	34
NC	NC NC	81	31

Table 1. Investigation of the tandem hydroformylation/acyloin reaction with other substrates. Reaction cond.: 6 mmol olefin, 0.03 mmol Rh(CO)2acac, 0.09 mmol Biphephos, 0.6 mmol thiamine•HCl, 2.4 mmol Et3N, 30 bar CO/H2 (1:1), 5 mL DMF, 60°C, 16 h. Results determined by GC in %.

In general, only acyloins, intermediate *n*-aldehydes and olefin isomers were observed after the reaction. 1-octene was applied as model substrate and yields 73% acyloins. Neohexene shows an excellent reactivity in hydroformylation reaction forming 98% *n*-aldehydes with an expected excellent regioselectivity giving 76% yield for the acyloin product. More interesting acyloin products are furnished by applying 5 hexenenitrile and methyl 10 undecenoate, a renewable derived from castor oil. The acyloin products contain a diester or a dinitrile moiety being interesting for polymer applications. Both substrates show increased isomerization activity which results in double bond isomers.

In summary, we described the first tandem hydroformylation/acyloin reaction yielding atom efficiently acyloins from olefins and syngas. We achieve an excellent *n/bra* ratio up to >99 with yields up to 98% for intermediate *n*-aldehydes and up to 76% for acyloins.

Contact:
Karoline.ostrowski@bci.tu-dortmund.de
thiemo.fassbach@bci.tu-dortmund.de
arno.behr@bci.tu-dortmund.de
andreas.vorholt@bci.tu-dortmund.de

Publications:
K. A. Ostrowski, T. A. Faßbach, A. J. Vorholt, Adv. Synth. Catal., in press, DOI 10.1002/adsc.201401031

Combination of homo- and heterogeneous catalysis in miniplant scale

Production of saturated branched fatty derivatives

Jennifer Haßelberg, Carsten Weiser, Jan B. Bially, Arno Behr

Branched oleo derivatives have a huge potential, particularly in cosmetics and lubricants industry which is based, among other advantages, on their low melting point and high thermal and oxidative stability. A process for the synthesis of saturated branched oleo derivatives from renewable raw materials and a new method for catalyst recycling were developed including a combination of homo- and heterogeneous catalysis.

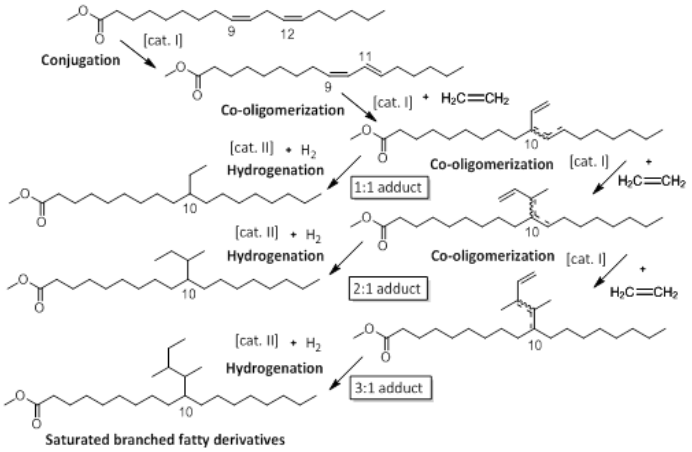

Fig. 1: Reaction sequence forming saturated branched fatty derivatives from linolenic acid methyl ester

Branched fatty derivatives can be formed from linolenic acid (methyl ester) by tandem reaction consisting of conjugation and co-oligomerization (Y=80%, t=5h) (Fig.1). A homogenous rhodium catalyst (c($RhCl_3$*3H_2O)=1mol%) is used which has to be recycled. Thermomorphic multicomponent solvent systems (TMS) are one solution for catalyst recycling. Therefore, due to coordination of the Rh-catalyst to the double bonds of the oleo compound (Fig.2) only 55% of the catalyst can be separated from the unsaturated product phase by TMS technique.

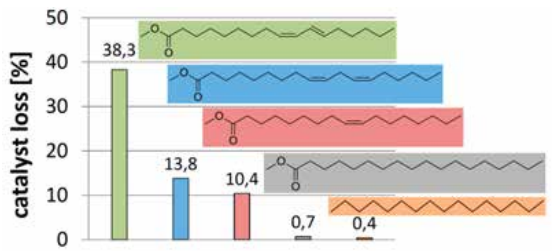

Fig. 2: Catalyst loss after extraction with propylene carbonate from several oleo compounds/n-hexadecane (m_{PC}:m_{oleo}=1:1,$T_{sep.}$=10°C)

For additional catalyst extraction a hydrogenation step is necessary. The developed process including hydrogenation and additional catalyst extraction is shown in Fig. 3 (left).

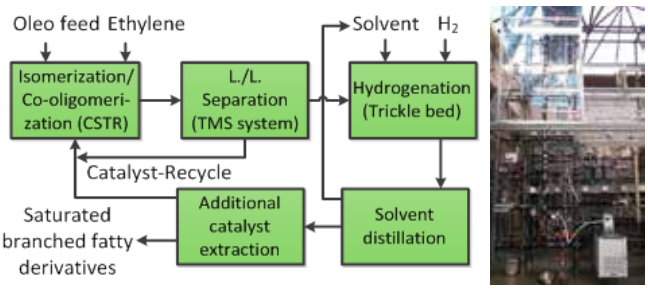

Fig. 3: Developed process for the production of saturated branched fatty derivative (left) and miniplant for hydrogenation (right)

Hydrogenation was investigated in miniplant scale using a trickle bed reactor with Pd/C1% as heterogeneous catalyst (Fig. 3 (right)). Rhodium was found to be partly adsorbed by the heterogeneous catalyst during hydrogenation.

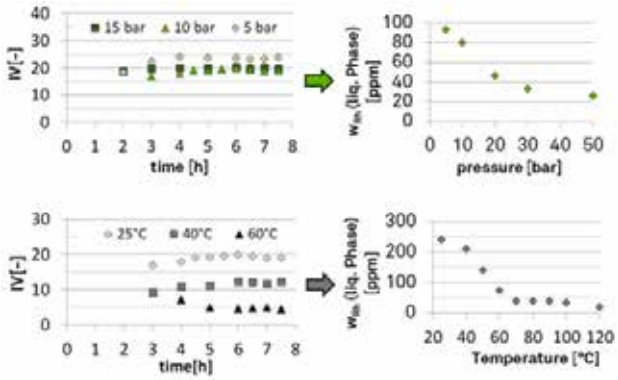

Fig. 4: Results of hydrogenation: Iodine value (left) and remaining rhodium content in liquid phase (right)

Rhodium adsorption to fixed bed shows unique reliance to reaction conditions and could be decreased from 76,3% to 9,6% (Fig. 4).
By additional rhodium extraction after hydrogenation the rhodium content of the product phase was reduced up to 2 ppm (0,2 w%).

Contact:
arno.behr@bci.tu-dortmund.de
jennifer.hasselberg@bci.tu-dortmund.de

Publications:
Behr, A.; Witte, H; Kämper, A.; Haßelberg, J.; Nickel, M.: Development and Investigation of the Production of Branched Oleo Derivatives in Miniplant Scale, In: Chemie Ingenieur Technik 86 (4), pp. 458–466, 2014
J. Haßelberg, A. Behr, C. Weiser, J.B. Bially: Combination of Homogeneous and Heterogeneous Catalysis in Miniplant Scale: New Process for Synthesis of Saturated Branched Oleo Derivatives. Oral Presentation: 106th AOCS Annual Meeting and Industry Showcases, Orlando/Florida, 2015

Highly selective iridium-catalyzed hydroformylation

Efficient catalyst recycling and scale-up into continuous miniplant operation

Alexander Kämper, Arno Behr, René Kuhlmann, Kristina Reiswich, Sirisap Jenny Warrelmann

Hydroformylation (oxo-synthesis) is one of the most important homogeneous catalyzed reactions in chemical industry and leads to a wide range of products e.g. solvents, plasticizers, odorants or fine chemicals. In the last centuries catalysts based on cobalt and especially rhodium, which is one of the scarcest and most expensive transition metals, has been established. For a more resource efficient prospect it is necessary to focus on alternative metals such as iridium including the opportunity for an industrial application. Therefore we developed a new appropriate and selective catalyst recycling concept with high catalytic performance which has been transferred successfully into continuous miniplant operation regarding examinations for catalytic long-term activity and stability.

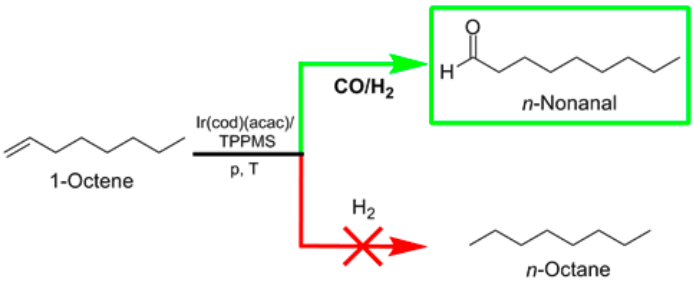

Figure 1: Hydroformylation of 1-octene (TPPMS = monosulfonated triphenylphosphine)

Often in homogeneous catalysis iridium-complexes are applied for selective hydrogenation reactions. However, in the present case it is necessary to suppress the hydrogenation for improving the hydroformylation performance (Figure 1). The addition of salts such as LiCl and a suitable range of CO/H_2 (2/1) lead to high chemoselectivities up to 94 % (*n/iso* = 75/25) towards the desired C_9-aldehydes while the conversion of 1-octene reaches a maximum of 93 % after 6 h.

Figure 2: Catalyst recycling via liquid-liquid separation

For an efficient catalyst recycling polar solvents such as *N,N*-dimethylformamide (DMF) have been established including thermomorphic solvent systems or an extraction with non-polar solvents. The extraction with 2,2,4-trimethylpentane lead to a very efficient catalyst recycling with 0.2 % iridium and 0.3 % phosphorous leaching while the product separation is at 80 % (Figure 2).

Based on semi-batch reactions and recycling experiments in lab-scale a continuously operated miniplant was projected, constructed and started-up (Figure 3).

Figure 3: Miniplant for hydroformylation with alternative transition metals

Parameters such as reaction temperature, pressure and CO/H_2 ratio have been optimized through continuous miniplant operations. In long-term experiments the catalytic activity and stability could be validated over a period of more than 90 h including high chemoselectivities and conversions up to 85 % (Figure 4).

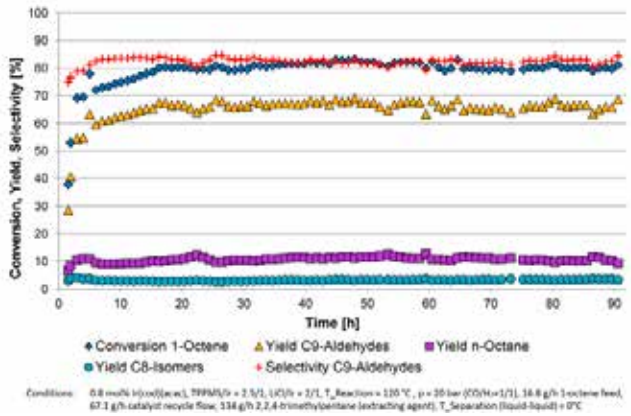

Figure 4: Iridium-catalyzed hydroformylation in continuous miniplant operation

Contact:
alexander.kaemper@bci.tu-dortmund.de
arno.behr@bci.tu-dortmund.de

Publications:
A. Kämper, A. Behr, P. Kucmierczyk, K. Reiswich, S. J. Warrelmann: Homogeneous catalyzed hydroformylation with alternative transition metals in miniplant scale. Poster: 48. Jahrestreffen Deutscher Katalytiker, Weimar, 2015.

Rhodium catalyzed one-step hydroamidation of cyclopentadiene and dicyclopentadiene

Direct route from alkene to amide

Denys Levikov, Edwad Nürenberg, Arno Behr

A direct one-step rhodium catalyzed route from alkene to amide is presented with the hydroamidation of cyclopentadiene and dicyclopentadiene, respectively, with pyrrolidine. A homogeneous Rh-catalyst without additional phosphorus ligand was established giving a 90% yield of monoamide species of Dcpd with a high Turn-Over-Frequency (TOF) of 1060 h^{-1}.

The carboxylic acid amide group is of great importance in the contemporary chemical and pharmaceutical industry. There can be found a variety of applications as industrial intermediates, fine chemicals and monomeric building blocks for polyamides. The state of art in amide bond formation is described well in some recently published reviews. The direct carbonylation of alkenes in the presence of amines to get amides, the so called hydroamidation (HAD), is an outstanding elegant synthesis way among them. The hydroamidation reaction can be subdivided in two types: the one- and the two-step-HAD (Figure 1).

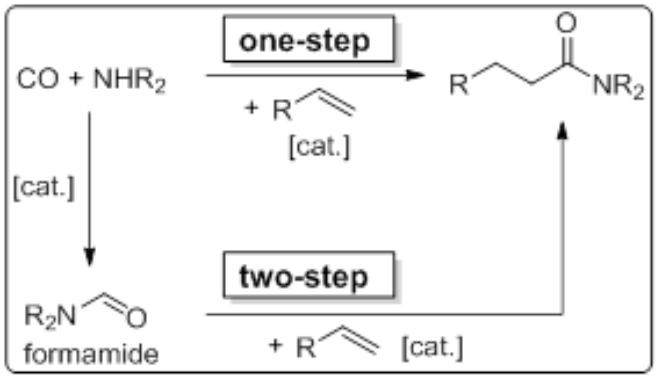

Figure 1. The two types of the hydroamidation reaction

The two-step-HAD involves a pre-synthesized formamide and an unsaturated compound without an external CO-atmosphere. The one-step-HAD is a one-pot synthesis of an alkene and an amine in presence of carbon monoxide. For our studies on the one-step-HAD the unsaturated basic chemicals cyclopentadiene and dicyclopentadiene, which make 25 weight% of the C5 fraction of the steamcracker, were chosen as starting compounds. Here we present a hitherto unknown, first rhodium-catalyzed derivatisation of dicyclopentadiene (Dcpd) outgoing from cyclopentadiene (Cpd) with the amide group by the one-step-hydroamidation reaction.

Looking forward to the amides of cyclopentadiene, only products of Dcpd were achieved. The monoamide 1 was selectively obtained in high yield, while for the formation of the diamide 2 a long reaction time was required.

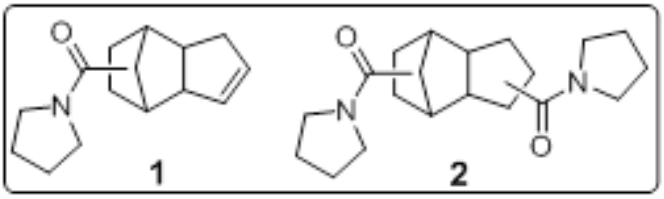

Figure 2. Mono- and diamide species of Dcpd

Amides of cyclopentadiene were not detected due to the long reaction time and high starting temperature needed for this reaction, which lead to a very fast dimerization rate of Cpd to Dcpd. Therefore, dicyclopentadiene was used directly as substrate. As a result of systematic screening we optimized the reaction conditions, which led to $[Rh(cod)Cl]_2$ as the best catalyst without any additional ligand giving 90% of Dcpd monoamide 1 with a high TOF of 1060 h^{-1} and over 90% selectivity within 1h. A partial polymerisation occurred during the reaction was successfully overcome with the use of low amounts of solvent and an optimized molar ratio of alkene to amine of 1:4.

Publications:
D. Levikov, E. Nürenberg, A. Behr, Rhodium catalyzed one-step hydroamidation of cyclopentadiene and dicyclopentadiene, Catalysis Science & Technology, 2015, DOI: 10.1039/C5CY00168D

Contact:
arno.behr@bci.tu-dortmund.de

Financial support from the Deutsche Forschungs-gemeinschaft (DFG) is gratefully acknowledged

Hydroformylation of renewables in an aqueous reaction system

Tom Gaide, Jens Dreimann, Andreas J. Vorholt, Arno Behr

A novel process concept for the hydroformylation of methyl 10-undecenoate is presented using an aqueous reaction system. This system consisting of water and 1-butanol enables an efficient and straightforward catalyst recycling via decantation of the product phase after reaction. The yield of the linear aldehyde is up to 74% using relatively mild conditions. A continuous operated miniplant process was established and the reaction was conducted for 20 hours without any loss of activity or selectivity and without any intervening in the process.

The implementation of renewable feedstocks like fatty acids or their methyl esters in industrial chemistry is of great interest due to the shortage of fossil fuels. One of the most important industrial scale applications of homogenous catalysis is the hydroformylation. The application of oleocompounds like methyl 10-undecenoate in this reaction leads to aldehydes, which are valuable intermediates for polymer synthesis (Figure 1).

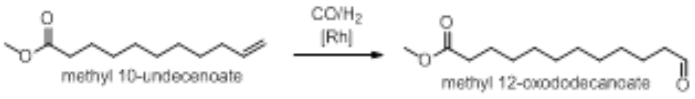

Figure 1: Hydroformylation of methyl 10-undecenoate

Recovery of the valuable noble metal catalyst is one of the main challenges in homogeneously catalysed reactions, especially if products with low vapour pressure and medium polarity are synthesised.

Herein we report a reaction system for the hydroformylation of methyl 10-undecenoate using a thermomorphic multicomponent solvent system (TMS) consisting of water and 1-butanol. The aqueous phase contains the catalyst built of $Rh(CO)_2acac$ as precursor and Sulfoxantphos as a water-soluble, bidentate phosphorous ligand and the alcoholic phase contains the substrate/product. Heating the mixture to the reaction temperature of 140 °C provides a highly efficient hydroformylation reaction. After reaction the solution is cooled down to room temperature and phases are separated.

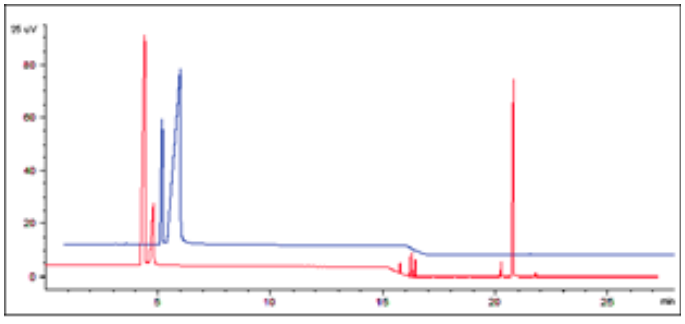

Figure 2: Chromatograms of the catalyst phase (blue) and the product phase (red)

The product phase contains more than 99% of the substrate and the formed aldehydes (see chromatograms in Figure 2). The loss of the precious catalyst with rhodium concentrations of 5 ppm and phosphorous concentrations of 2 ppm in the product phase is very low.

Best results in laboratory scale batch experiments were observed using one hour reaction time, relatively low catalyst concentrations (0.1 mol% rhodium-precursor, 0.5 mol% Sulfoxantphos) and moderate synthesis gas pressures (20 bar, CO/H_2:1/1). With this reaction system high yields of the linear aldehyde (70%) and high linear/branched ratios (90/10) are achievable. Because the catalyst phase could be reused up to three times without any loss of activity or selectivity, the reaction was transferred into miniplant scale.

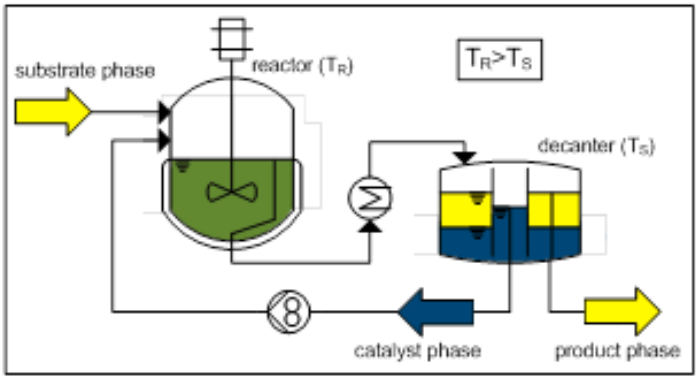

Figure 3: Flow diagram TMS-miniplant

A continuously operated hydroformylation process could be realised for a reaction time of 20 h with a yield of 74% of the linear aldehyde without any intervening in the process.

This work is part of the DFG Sonderforschungs-bereich Transregio 63 (SFB/TRR63) InPROMPT. Financial support by the Deutsche Forschungs-gemeinschaft (DFG) is gratefully acknowledged. We thank the Umicore AG&Co.KG for the donation of the rhodium precursor.

Contact:
tom.gaide@bci.tu-dortmund.de
jens.dreimann@bci.tu-dortmund.de
arno.behr@bci.tu-dortmund.de
andreas.vorholt@bci.tu-dortmund.de

Hydroaminomethylation of limonene with aqueous ammonia

Atom economic synthesis of a primary amine from a natural compound

Arno Behr, Andreas Wintzer

Primary aliphatic amines are important products in the chemical industry. They provide useful properties for application and are also important intermediates for further fine and pharmaceutical chemicals. The direct synthesis of these com-pounds from alkenes with ammonia as substrate is a big challenge for primary amine selectivity. With the hydroamino¬methylation of the natural resource limonene with ammonia a direct route for the synthesis of a primary amine is presented.

The hydroaminomethylation (HAM) is a tandem reaction which consists of three different reactions that take place consecutively: after the hydro-formylation of an alkene the aldehyde reacts in a condensation reaction with an amine substrate (ammonia) giving an imine which is finally hydrogenated. In the HAM of limonene, due to the reaction conditions, a few side reactions can occur (Figure 1). Besides the hydroformylation in the first step the active double bond can be hydrogenated or rearranged as the target molecule is able to build higher molecular substrates.

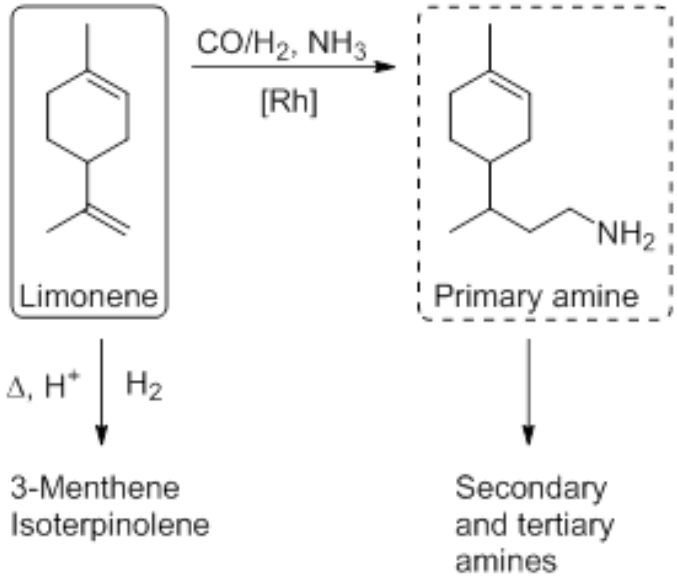

Figure 1. Reaction scheme of the HAM of limonene with possible side reactions.

As can be seen in the reaction scheme, the side reactions need to be suppressed to achieve an optimum yield of the primary amine. Therefore a biphasic solvent system was used, which consists of an aqueous ammonia containing catalyst phase and an organic educt/product phase (toluene as solvent). It turned out that the mainly occurring side reaction is the isomerisation of limonene to isoterpinolene.

Resulting from experience with similar reactions [Rh(cod)Cl]$_2$/TPPTS (TPPTS = Triphenylphosphine trisulfonate) was chosen as catalyst system.[1] The constitution of the catalytic system, the precursor concentration and the rhodium/phosphine ratio proved to be important reaction parameters (Table 1). A large ammonia excess of up to a NH_3/limonene ratio of 36 was shown to be counter-productive, whilst an 8-fold excess in combination with other optimised reaction conditions yielded in best results.

NH_3/ Limonene	c (precursor) [mol%]	[Rh]/P	Primary Amine	Isoterpinolene
8	0.5	1:8	4%	51%
16	0.5	1:8	14%	33%
8	0.2	1:4	19%	36%
8	0.2	1:8	21%	31%
8	0.5	1:4	25%	28%

Table 1. Optimised reaction conditions for the HAM of limonene. Reaction conditions: 6 mmol limonene, 5.84·10-3 mol·l-1 CTAC, 5 ml toluene, 800 rpm, 130 °C, 60 bar CO/H2, 6 h.

In addition, for good results in terms of primary amine yield a high synthesis gas pressure of 60 bar is necessary. In contrast to recent experiences in the reductive amination of citronellal, the surfactant CTAC (Cetyltrimethylammonium chloride) is offering a good phase separation after the reaction. A maximum yield of 25% of the primary amine can be achieved. At the same time the isomerisation from the starting material can be suppressed effectively from 51% to 28%. These optimized reaction conditions provide a good base for the direct synthesis of a high value fine chemical from a natural resource.

Financial support from the Deutsche Forschungsgemeinschaft (DFG) is gratefully acknowledged.

Publications:
A. Behr, A. Wintzer, From Terpenes to Amines: A Critical Review, in: J. Hu (Ed.), New Developments in Terpenes Research, Nova Science Publishers, New York, 2014, pp. 113-134

Contact:
arno.behr@bci.tu-dortmund.de
andreas.wintzer@bci.tu-dortmund.de

Novel Telomerisation of Piperylene with Morpholine

Convenient access to branched C_{10}-amines

Peter Neubert, Ines Meier, Tom Gaide, Rene Kuhlmann, Arno Behr

Here, we present the first telomerization of piperylene with morpholine, which provides atom economic access to unsaturated C_{10} amines in a single reaction step. Screening of several reaction parameters revealed $Pd(acac)_2$/IMes·HCl as the most active catalyst under mild conditions. At 100°C up to 83% of the tail-head telomer can be obtained within five hours.

In the course of diminishing fossil feedstocks, one major goal of catalysis is the development of efficient synthesis routes based on well-known, yet unutilized compounds. Among those, there is piperylene (1,3-pentadiene) 1 (figure 1) which can be easily obtained from the C_5-fraction of the steamcracker. Today, after hydrogenation and isomerization it is used as a gasoline additive.

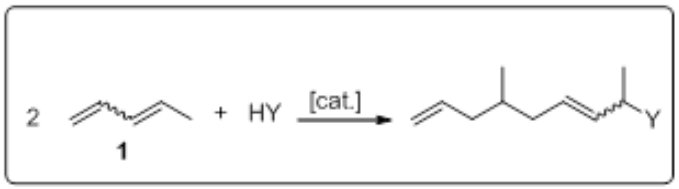

Figure 1. General equation of piperylene telomerization.

A convenient access to functionalized long chain olefins is the telomerization reaction in which two dienes react with a feasible nucleophile (figure 1). The products may be used in fine chemistry, or in the production of polymers and surfactants.

By now, other dienes such as butadiene and isoprene have been widely examined in telomeri-zations; in contrast, piperylene has been investigated rarely. To the best of our knowledge, to date there is no telomerization of piperylene with amines.

The desired main product is the tail-head telomer 4. In a 1:1 side reaction, hydroamination products 3a/b have also been observed, as well as piperylene dimers, e.g. compound 2 (figure 2).

In our investigations we were focused on the conversion with catalysts derived from a palladium species and a strongly binding carbene ligand. The active species forms by simple addition of palladium salt such as $Pd(acac)_2$ and the carbene hydrochloride in the presence of a suitable base.

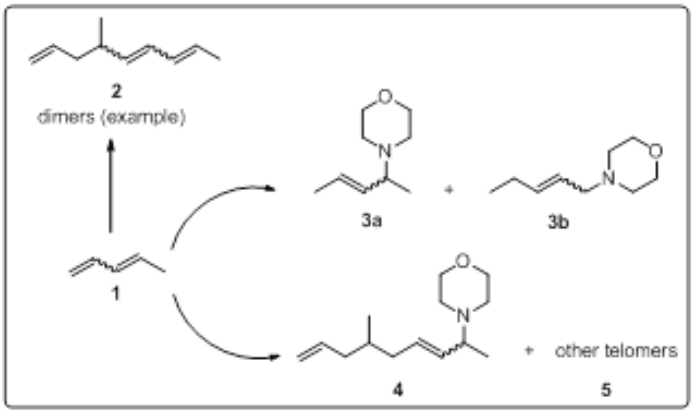

Figure 2. Product scheme

Screening of the catalyst led to: 0.2 mol% $Pd(acac)_2$ and Imes HCl in a 1:2 ratio as the best conditions [Imes = 1,3-bis (2,4,6-trimethylphenyl)-imidazolium]. Furthermore, the addition of the base is crucial for ligand activation only. We have conducted experiments with the free carbene ligand, without base, which also provided telomer yields up to 78%. However, in situ formation from the hydrochloride is much more convenient, as the free carbene is very sensitive to air and moisture.

Finally, the conduction of time dependent experiments exhibits, that after five hours the reaction provides 83% of the telomer 4 in a high selectivity of 91%.

Contact:
arno.behr@bci.tu-dortmund.de

Publications:
P. Neubert, I. Meier, T. Gaide, R. Kuhlmann, A. Behr, First Telomerisation of Piperylene with Morpholine using Palladium-Carbene Catalysts, in preparation.

Thermodynamics (TH)

Estimating protein interactions in ATPE based on osmotic virial coefficients

Identifying suitable displacement agents for selective protein purification

Christian Kress, Christoph Brandenbusch, Gabriele Sadowski

Aqueous two-phase extraction (ATPE) enables the purification of proteins under mild and biocompatible conditions. Commonly, in order to allow for a selective partitioning of the target protein within the ATPE, a displacement agent (e.g. salt) is used. In this work, the selection of a suitable displacement agent was carried out by means of the molecular interactions between the proteins and solutes in solution. In detail, the osmotic cross virial coeffient B_{23} was used to access the interactions between the target protein (immunoglobulin G) and the impurity (human serum albumin) with different solutes (phase formers and displacement agents). This allowed for designing an extraction system suitable for selective purification of target proteins.

In this work, the partitioning behavior of the target protein immunoglobulin G (IgG) and the impurity human serum albumin (HSA) was determined in an aqueous two-phase system (ATPS) in the absence of a displacement agent as illustrated in Fig. 1a. As shown in Fig. 1b, both proteins tend to be exclusively (>96%) distributed to the bottom phase. To achieve selective partitioning of IgG, a suitable displacement agent (e.g. salt) had to be found.

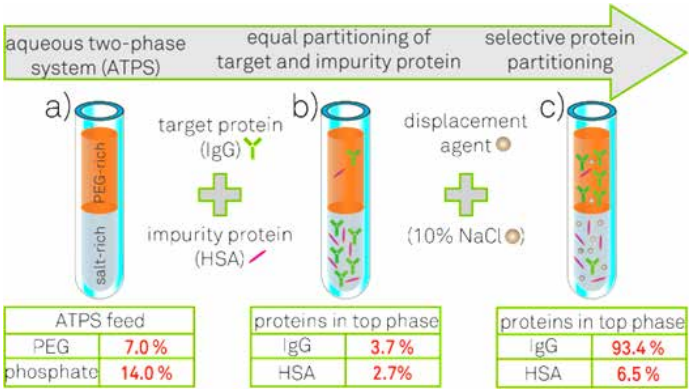

Figure 1: Schematic illustration of the partitioning behavior of immunoglobulin G (IgG) and human serum albumin (HSA) within an ATPS composed of 7%PEG2000 and 14% phosphate buffer at pH 7 and 25°C. A selective purification of both proteins is realized based on an addition of 10% NaCl. a) NaCl-free, protein-free ATPS; b) ATPS upon addition of IgG and HSA; c) ATPS from b) upon addition of 10% NaCl

Suitable displacement agents were assumed in this work to be characterized by high B_{23} values which are caused by strong repulsive interactions between the protein and the displacement agent. These B_{23} values were determined based on static light scattering. As illustrated in Fig. 2, all B_{23} values show values greater than zero representing repulsive protein-solute interactions in solution at 25°C and pH7.

As the B_{23} value between IgG and NaCl is significantly higher than the B_{23} of HSA and NaCl, NaCl is expected to be a suitable displacement agent allowing for a separation of the two proteins using an ATPS. This estimation was experimentally validated by adding 10% NaCl to the initial ATPS which dramatically changed the partitioning of IgG compared to HSA. The amount of IgG in the top phase increased up to 93.4% whereas the amount of HSA in the bottom phase remained almost constant (see Fig.1c). These results confirm that NaCl is a suitable displacement agent providing a selective purification of the two proteins.

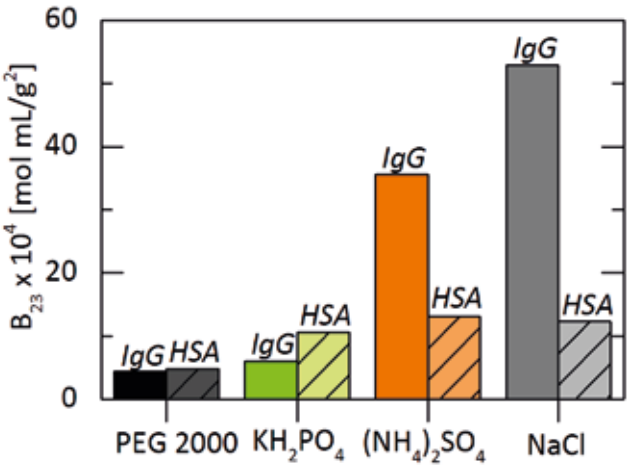

Figure 2: Cross virial coefficient B_{23} between protein (IgG and HSA) and different solutes in an aqueous 0.05 M K_2HPO_4-NaH_2PO_4 buffer solution at pH 7 and 298.15K

In summary, a new approach for the estimation of protein interactions in ATPS based on osmotic virial coefficients was developed. The results shown elucidate that the cross virial coefficient B_{23} is helpful to find suitable displacement agents that enable selective protein partitioning in ATPE processes.

Contact:
christian.kress@bci.tu-dortmund.de
christoph.brandenbusch@bci.tu-dortmund.de
gabriele.sadowski@bci.tu-dortmund.de

Publications:
Kress, C.; Brandenbusch, C., Osmotic Virial Coefficients As Access to the Protein Partitioning in Aqueous Two-Phase Systems, Journal of Biotechnology and Bioengineering submitted 2015

Solvent Effects on Reaction Equilibria

Quantitative Prediction of Solvent Effects on Esterification Reactions

Ole Riechert, Tim Zeiner, Gabriele Sadowski

Solvents built the environment for liquid-phase reactions and therewith influence reaction kinetics, reaction equilibrium, and yield. A thermodynamic modeling approach was applied to predict the effects of solvents and solvent mixtures on the reaction equilibrium of the esterification of ethanol and acetic acid. Effects of various solvents and mixtures thereof on equilibrium concentrations of the reaction were predicted in excellent agreement with experimental data. Predictions were performed solely based on the knowledge of phase-equilibrium data without fitting any parameters to the reacting system.

The thermodynamic equilibrium constant K_a does neither depend on reactant concentrations nor on solvents - it is a function of temperature only. In contrast, the mole-fraction-based apparent equilibrium constant (K_x) depends on reactant concentrations as well as on solvents as shown for the esterification of acetic acid and ethanol in Fig.1.

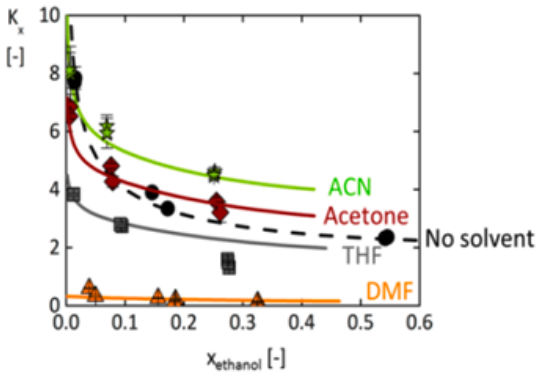

Figure 1: K_x of ethanol/acetic acid esterification as function of the equilibrium mole fraction of ethanol at 313.15 K and atmospheric pressure in the solvent-free system (dashed line) and in different solvents (solid lines; solvent mole fractions are 0.5). Symbols are experimental data and lines are predictions with PC-SAFT.

In the solvent–free system, high ethanol concentrations suppress the reaction (low K_x values), whereas low ethanol concentrations (high acetic acid concentrations) support the reaction, leading to high K_x values.

K_x is related to the equilibrium constant K_a by Eq.(1)

$$K_x = K_a / K_\gamma \quad (1)$$

The activity-coefficient contribution K_γ is obtained from activity coefficients of reactants and products and depends on reactant concentrations and on solvent(s) and so does K_x.

Modeling the activity coefficients with PC-SAFT and using K_a allowed for predicting K_x from Eq. (1) (see Fig.1).

Herein, PC-SAFT model parameters were estimated based on binary systems' phase-equilibrium data only. None of the parameters was fitted to reaction data.

To predict solvent effects, the modeling approach was extended to describe reactions in solvents. PC-SAFT parameters were fitted to phase-equilibrium data of binary systems containing reactants/products and a solvent. PC-SAFT predictions of K_γ and therewith of K_x revealed that acetonitrile (ACN) supports the esterification whereas it is suppressed by tetrahydrofurane (THF) and dimethylformamide (DMF). These predictions are in excellent agreement with the experimental observations (Fig.1).

Finally, the developed approach was extended to esterification in solvent mixtures. For all considered solvent mixtures composed of ACN and/or DMF, the experimentally-observed trend of K_x values could be predicted almost quantitatively (Fig.2).

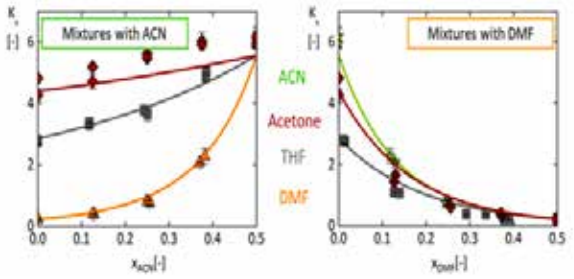

Figure 2: K_x of ethanol/acetic acid esterification at 313.15 K and atmospheric pressure in solvent mixtures with ACN (left) and DMF (right) as function of the mole fraction of one solvent (overall solvent mole fraction of 0.5). Symbols are experimental data and lines are predictions with PC-SAFT.

The developed approach considers the physics of the reactants/products and solvents and is thus a valuable tool for predicting the solvent influence on the equilibrium concentrations of equilibrium reactions.

Publications:
Riechert, O.; Zeiner, T.; Sadowski, G., Solvent effects on esterification reaction equilibria, AIChE Journal submitted 2014
Riechert, O.; Zeiner, T.; Sadowski, G., Solvent effects on reaction equilibria of homogeneous esterification reactions, AIChE Annual Meeting, Atlanta, USA (204)

Contact:
ole.riechert@bci.tu-dortmund.de
tim.zeiner@bci.tu-dortmund.de
gabriele.sadowski@bci.tu-dortmund.de

Analytical Modeling of Appendix Gap Losses in Stirling Cycle Machines

Jens Pfeiffer, Hans-Detlev Kühl

The thermal losses caused by an annular gap between the insulating dome of a piston and the adjacent cylinder wall in a Stirling engine, commonly referred to as appendix gap losses, amount to approximately 10 % of the heat input. In this research work, a new analytical model for these losses has been developed, since previous modeling approaches are based on rather gross and partly questionable assumptions and therefore appeared to be insufficient.

A typical cylinder system in a Stirling cycle machine, as shown in Figure 1, works between two temperature levels. To minimize thermal conduction, the displacer is designed as a long, thin-walled dome. To protect the piston seal from the hot temperature, it is mounted at the cold, near-ambient temperature. This inevitably leads to an annular gap of width *h* around the displacer, which is commonly referred to as the appendix gap.

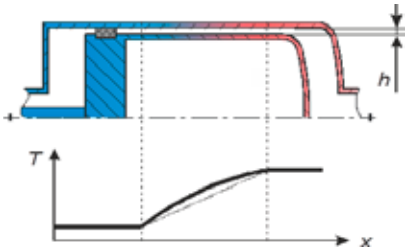

Figure 1: Cross section of the cylinder-displacer system in a Stirling cycle machine, and the assumed temperature profile along the gap.

Beside wall heat conduction, two gap loss mechanisms have to be considered: First, the shuttle heat transfer in fact is a cyclic radial heat transfer caused by the relative displacement of the cylinder and displacer wall tempera-ture profiles. An increased width of the gap, which forms an insulating layer between both walls, reduces this loss. Second, the cyclic mass flow along the gap causes a net enthalpy flow, which is enlarged by increasing the gap width. Therefore, an optimum gap width exists.

An extensive review has revealed that previously existing gap loss models are partly based on questionable as-sumptions and therefore are of limited accuracy. Hence, a new model has been developed within this research work, which was formulated analytically to identify the main dependencies on the design parameters.

For the new gap model, analytical solutions for the flow pattern and the gas temperature profile have been directly derived from the unsteady Navier-Stokes and energy equations. Whereas previous models assume a pure drag flow in the gap, the present model considers an additional pressure-driven flow component, which is evidently present due to the volumetric displacement by the piston seal and the compression and expansion of the enclosed gas. Herewith, a more accurate solution for the shuttle heat transfer could be derived. In previous models, the net enthalpy flow was evaluated at the open end of the gap, and the assumptions for the bulk gas temperature appear arbitrary in some respect. With the solutions for the flow pattern and the temperature profile, a closed-form expression for net enthalpy flow could also be derived, which does not require any additional assumptions.

In this work, the loss mechanisms have been investigated with respect to their dependency on the gap position, and a curved cylinder wall temperature profile (Figure 1) could be identified, which corresponds to previous numerical simulation results and experimental findings. Using the data of a well-documented Stirling engine, Figure 2 shows a plot of the gap loss vs. the gap width according to previ-ous (dashed lines) and present (solid Line) model predic-tions. The optimum predicted by this model is at a far smaller gap width and agrees well with the actual value ($h^* = 1$), which probably was optimized experimentally. Furthermore, the present model predicts higher losses. This agrees with experimental heat balance data.

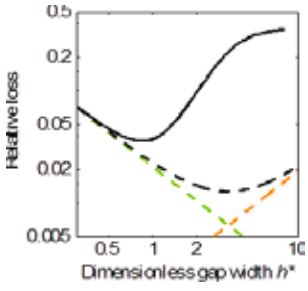

Figure 2: Shuttle heat transfer (green line), net enthalpy flow (orange line) and overall gap loss (black lines) vs. the gap width for previous models (dashed lines) and the new model (solid line).

The enhanced accuracy of this model for the cylinder system in Stirling cycle machines allows a well-founded optimization of the gap geometry and may therefore help to further improve their efficiency in future.

Contact:
jens.pfeiffer@tu-dortmund.de
hans-detlev.kuehl@bci.tu-dortmund.de

Publications:
J. Pfeiffer, H.-D. Kühl; New Analytical Model for Appendix Gap Losses in Stirling Cycle Machines; Journal of Thermo-physics and Heat Transfer, (submitted 2015).
J. Pfeiffer, H.-D. Kühl; Review of Models for Appendix Gap Losses in Stirling Cycle Machines, Journal of Propulsion and Power 30 (5), 1419-32 (2014).

Salt influence on liquid-liquid equilibria of aqueous/organic systems

Measuring and predicting salting-in and salting-out effects on 5-Hydroxyfurfural (5-HMF)

Sultan Mohammad, Christoph Held, Gabriele Sadowski

Salts are involved in many chemical and especially biological processes, such as in the production of organic molecules. In this work the salt influence on liquid-liquid equilibria of MIBK (methyl isobutyl ketone)/water and MIBK/water/5-HMF systems was investigated. All salts caused salting-out of MIBK from the aqueous phase. Unexpectedly both, salting-in and salting-out effects, were observed for 5-HMF from the aqueous phase, depending on the kind and concentration of the salt. This experimentally-observed behavior could be predicted quantitatively with electrolyte PC-SAFT (ePC-SAFT).

Knowledge of liquid-liquid equilibria (LLE) of organic solvent/water/biomolecule systems is required for optimization of extraction steps in production processes of biomolecules. In those processes, salts might be present due to intentional addition or due to presence in the reaction media. In this work, the influence of various salts on the LLE in the system MIBK/water was investigated.

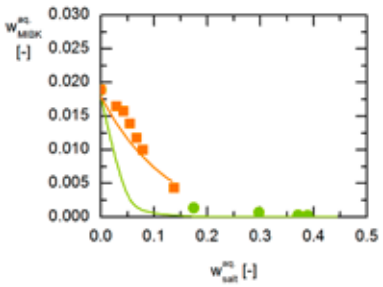

Figure 1: LLE in MIBK/water/salt systems. Equilibrium weight fraction of MIBK in the aqueous phase vs. equilibrium weight fraction of salt until salt solubility limit at 298.15 K and 1 bar. Circles (LiCl) and squares (Na_2SO_4) are experimental results. Lines are modeling results with ePC-SAFT.

For all systems considered, salt was mainly present in the aqueous phase, whereas only small amounts were found in the MIBK phase. Considering the experimental weight fractions of MIBK in the aqueous phase revealed that MIBK was salted-out from the aqueous phase upon addition of all salts under investigation. The strength of the salting-out effect follows the order LiCl>NaCl>KCl. Concerning the anions, the salting-out effect increased in the order NO_3^-<CH_3COO^-<Cl^- ≈SO_4^{2-} regardless of the cation. As an example, it can be seen from Figure 1 that LiCl causes a stronger salting-out on MIBK from the aqueous phase than Na_2SO_4. Applying the model ePC-SAFT allowed for satisfactorily describing this behavior (Figure 1).

The influence of salts on the system MIBK/water/5-HMF and the partitioning of 5-HMF between aqueous and MIBK phases is of great interest in academia and in industry in order to optimize extraction processes of 5-HMF.

The experimental distribution coefficients of 5-HMF ($K_{HMF} = w_{HMF}^{MIBK} / w_{HMF}^{aq.}$) in the absence of salt ($m_{salt} = 0$ in Figure 2) were found to be close to unity, meaning an almost equal distribution of 5-HMF between the aqueous and MIBK phases.

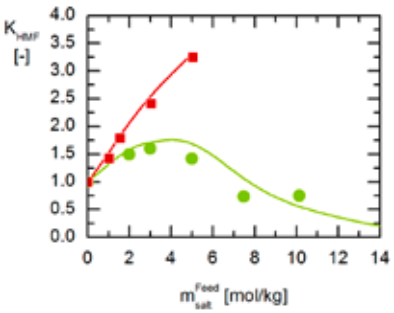

Figure 2: Distribution coefficients of 5-HMF in the system MIBK/water/5-HMF at 298.15 K and 1 bar as function of added salts. Circles (LiCl) and squares (CH_3COOLi) are experimental results. Lines are ePC-SAFT predictions.

The addition of a salt has a big impact on the distribution of 5-HMF between MIBK and water as shown in Figure 2 for the addition of LiCl and CH_3COOLi. As expected, a strong salting-out effect is observed upon addition of CH_3COOLi (K_{HMF}>1) and of small amounts of LiCl (<3mol/kg). Unexpectedly, addition of higher amounts of LiCl causes a salting-in effect (K_{HMF}<1) That is, the K_{HMF} values depend on both, kind and concentration of the salt added. ePC-SAFT was able to even accurately predict this behavior without parameter fitting. It was found that LiCl causes a chaotropic effect at high LiCl concentrations allowing 5-HMF to better fit into the water structure, which was well-captured by the model.

Publications:
C.Held, T. Reschke, S. Mohammad, AF. Luza, G. Sadowski, Chemical Engineering R&D 2014, 92, 2884-2897

Contact:
sultan.mohammad@tu-dortmund.de
christoph.held@tu-dortmund.de
gabriele.sadowski@tu-dortmund.de

Impressum

Fakultät für Bio- und Chemieingenieurwesen
TU Dortmund

www.bci.tu-dortmund.de

Redaktion: Prof. Jörg C. Tiller